Records of past climate obtained from study of glacial ice cores and other sources of proxy data indicate that global temperature and accompanying climate patterns have varied naturally over the past 10,000 years (Albritton et al. 2001; Denton and Karlen, 1973; Porter and Denton, 1967). However, the rate of global temperature change is predicted to accelerate over the next century in response to a continued rise in atmospheric greenhouse gas concentrations, resulting in an amplification of climate change that exceeds the natural pattern of variability (Albritton et al. 2001; Oldfield, 2004). Observation of the paleorecord has revealed that increased global temperature is followed by periods of increased frequency and magnitude of storms in many parts of the world (Bates et al. 2008). The resulting impact on river basins has been observed in sedimentological evidence of increased frequency and magnitude of flood events. A history of past flooding in a river basin based on analysis of overbank flood deposits can aid in the prediction of future hydrologic response of river basins to climate change resulting from global temperature increase. Three sediment cores obtained from overbank flood deposits preserved within the Utica Marsh in central New York were dated and analyzed for changes in bulk density, magnetic susceptibility, percent organic matter, percent carbonate and percent grain size to ascertain if they are indicative of flood events on the adjacent Mohawk River. Grain-size analysis revealed increases in sand-sized percentages indicative of high energy conditions occurring near in time to dated flood events. However, not all flood events are represented by a peak in sand. Thus these results suggest that floodplain deposits preserved in the Utica Marsh can be used to reasonably reconstruct a history of flooding on the Mohawk River pre-dating anthropogenic influence in the study area, but must be interpreted with caution.

A POTENTIAL RECORD OF RECENT FLOOD EVENTS PRESERVED IN UTICA MARSH SEDIMENT

by

Tamara L. Hughes

A Research Project Submitted to the Faculty of

Utica College

May 7, 2009

In Partial Fulfillment of the Requirements for the Degree

Master of Science

Table of Contents

List of Figures and Tables

Acknowledgements

I would like to thank my friends and family- particularly my husband Mike and children Ryan, Nathan and Jennifer- for all their love and support throughout my seemingly endless college career. I'm also grateful to my professors at Utica College for their guidance over the years, especially Drs. David Moore and Curtis Pulliam for their time and interest as committee members and Drs. Terri Provost and Thomas McCarthy for their assistance in the core collection. Many thanks also to Mike Washburn for his assistance with fieldwork in the Marsh. Finally, I wish to thank Dr. Sharon Kanfoush for her role as Committee Chair, patiently mentoring, critiquing and prodding me to the finish.

Introduction

Paleoenvironmental research is the study of past environments by means of data obtained from proxies, natural materials that preserve measurable evidence of previous environmental conditions. The analysis of proxy data archived in tree rings, plant and animal macrofossils, glacial ice cores and sediment profiles has revealed the nature of processes that shaped past environments (Albritton et al. 2001; Petit et al. 1999). Application of these methods has also increased our understanding of factors contributing to present-day environmental problems as well as their future implications (Brenner et al. 2001; Oldfield, 2004).

Of particular concern are the dramatic increase in concentration of atmospheric carbon dioxide and other greenhouse gases over the past 150 years and the accompanying rise in global temperature. Global temperature increase is predicted to impact other aspects of future climate, particularly the frequency and intensity of storms and resulting flood events (Albritton et al. 2001; Bates et al. 2008). Because such a large percentage of the world's population lives in close proximity to river basins, floods have the potential to seriously impact human welfare (Albritton et al. 2001). Consequently, the prediction of future hydrologic response of river basins to increased frequency and intensity of storminess associated with global temperature increase has become a serious focus of paleoenvironmental research (Knox, 2000; Bates et al. 2008).

The character of river and floodplain sediments reflects the nature and intensity of the processes by which they were deposited (Knox, 2000). Because the hydrologic processes of stream flow and sediment transport are influenced by environmental factors such as climate, observable sediment features can be proxies of past climate and other environmental conditions (Wolfe et al. 2006; Sant et al. 2004, Knox, 2000). In this way, specific changes in characteristics such as grain size, magnetic properties, organic content and other parameters within dated sediment layers can be identified and correlated with specific past events such as floods (Huang et al. 2007). If sediment layers remain undisturbed by tectonic forces and human activity, an extensive stratigraphic record of past climatic conditions and related river basin response can be preserved in river basin sediments (Sant et al. 2004). Sediment records long enough to pre-date human settlement of a region can also be used as a baseline and means to determine the extent to which a river basin has been affected in the past by agriculture, industrial development, flood control practices and other human activities, as well as the synergy of anthropogenic activities with environmental factors such as global warming (Wolfe et al. 2005). Sediment cores, then, can be used to ascertain if and how the frequency and magnitude of flooding has increased over the time span of anthropogenic global warming.

The principle objective of this study is to ascertain if it is possible to extract evidence of past flood events from overbank floodplain sediments deposited by the Mohawk River in the Utica area of central New York (Figure 1). As a floodplain, the sediments of the Utica Marsh should preserve evidence of past flood events on the Mohawk River and man-made barge canal (Sant et al. 2004, Knox, 2000). Chronological dating of sediments recovered by coring will enable the comparison of specific sediment characteristics with known flood events that impacted this area over the past 100-150 years. If flood events can be identified with confidence from the sediment features, this study will lay the foundation for the reconstruction of a much longer record predating the existence of instrumental records. Such a record could be used as a baseline with which to compare more recent trends and will help address the question of whether or not the frequency and magnitude of Mohawk River flood events have changed and whether this change was in response to global warming.

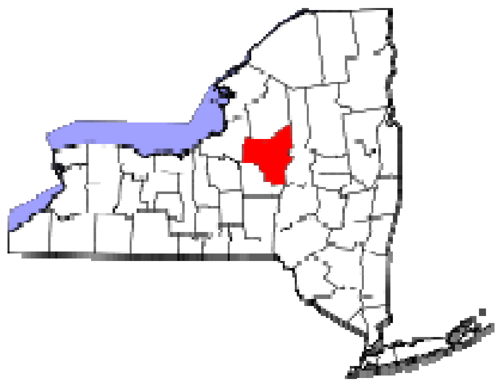

Figure 1: Map of New York State showing the approximate location of Oneida County, within which the Utica Marsh is located (Wikipedia, 2009).

Previous Studies

A recent trend toward an increase in recurrence frequency and magnitude of floods since the 1950s in many regions of the United States has been attributed to changes in land use (Knox, 2000; Schneider et al. 2007; Van Huissteden and Kasse, 2001). However, many studies have also shown a correlation between modern large-scale flood events and their resulting sediment signatures with instrumentally-measured atmospheric conditions in existence at the time of the event's occurrence (Hassan, 1981; Ely et al.1993). Paleoflood evidence, including radiocarbon-dated debris and alluvium in paleochannels and recent instrumental climate records, provided evidence for the proposed linkage between global warming and increased frequency of large overbank floods. Results of Knox (2000) showed a correlation between increases in flooding recurrence and changes in major atmospheric circulation patterns. These changes affected storm track trajectories, as well as the location and moisture content of air masses, resulting in rapid temperature changes and increased rainfall. Paleoflood evidence suggests that such climate-driven changes in flood frequency were often synchronous across large areas of the country. Although the Knox (2000) study was focused on river basins in the midwestern and southwestern regions of the country, it nonetheless supported the possible impact of global temperature increase on climate changes resulting in increased magnitude and frequency of large floods. It also illustrated the use of alluvial sediment features in flood history reconstruction.

An extensive record (580 cm) of unstratified floodplain sediments in tropical India dating between 30ka and 10ka was analyzed by Sant and others (2004) for evidence of shifts in major monsoonal events. Shifts in mean grain size and variability (standard deviation) of both the fine sand (>149 µm) and silt faction (<25 µm) as well as magnetic, mineral, calcite and carbonate properties within the sediment layers served as proxies for aeolian and fluvial depositional processes. Chronology of the sediment layers was established by correlation with luminescence dated records obtained from another location within the basin as well as Chinese loess plateau records and $\delta^{18}O$ records from the Guliya ice core located on the Tibetan Plateau in China. Sediment signals indicative of transitions from aeolian to flooding events (dry to wet periods), including the Last Glacial Period-Holocene transition and several oscillations between strong and weak monsoon periods, were represented within the floodplain record by shifts in the percentages of fine sand (>149 µm) and silt factions (<25 µm). These results suggest that floodplains in regions of low tectonic activity are capable of preserving proxy evidence of changes in continental processes signaling major climate events such as monsoonal rainfall and major droughts.

Sedimentary records of paleofloods are often incomplete due to erosion by subsequent flood events and human activities such as agriculture (Benito, 2003). Yet, based on an investigation of an alluvial plain along the middle reaches of the Yellow River in northern China, Huang and others (2007) provided evidence that flood deposits interspersed between loess and soil sequences were preserved from erosion and archived a complete record of large-scale floods extending well into the Holocene period. Sedimentary profiles exposed along gully banks, road beds and in archeological trenches were analyzed for variations in grain size, magnetic susceptibility and geochemical composition. Results revealed thin alluvial deposits interspersed between loess and paleosol layers. Stratigraphic evidence of six extreme episodes of overbank flooding were dated by means of ^{14}C or archeological evidence (ie. pottery shards) found within the layers and correlated with flood events documented in historical records and literary accounts of that region. Further comparison of proxy climate records and recent meteorological data suggest that the six Holocene flood events resulted from an anomalous large-scale circulation change that produced a shift between the southeastern and northwestern monsoon systems. The resulting atmospheric circulation pattern was likely similar to that which produced a series of unusually heavy rainstorms and overbank floods during the summer of 1958 in the same region. The results of this study support the hypothesis that extreme floods are produced by unique large-scale atmospheric circulation patterns and their effect on storm tracks and air masses (Knox, 2000).

White and Rodbell (2000) obtained a 1000-year long flooding record of the Mohawk River from the basin sediments of Collins Lake, an oxbow lake located within the river floodplain 78 miles east of Utica. An oxbow lake is the remainder of a meander left behind when a river changes course to cut a straighter channel. If the main source of sediment for an oxbow lake is the river from which it was formed, evidence of river flood events large enough to reach the lake should be preserved within its sediments (Winter et al. 2001). Characterization of the sediment layers within two radiocarbon dated cores revealed laminae consisting of alternating pink and brown silt layers. Physical and geochemical analyses identified three types of sediment differing in grain size and organic content. It was determined that covariation of distinct brown and pink silt layers (the fine-grained pink layers likely being formed from suspended river sediment and the coarser-grained brown layers primarily from river bedload) represented large-scale flood events that occurred during a time of increased storminess corresponding to the Little Ice Age (1180-1600). A sharp decrease in total carbon and increase in organic carbon observed in one core may be indicative of one of the last high magnitude (6m) floods on the Mohawk River in 1996. Similar decreases in carbon observed in the second core, as well as a spike in sand-sized grains at the top of the sequence, correlate with records of a wet period in the Northeast from 1840 to 1915 (White and Rodbell, 2000).

Flood history reconstruction is often used in the assessment of the impact of land use changes and watershed disturbances as well as climate influence on a river basin. For example, White and Rodbell (2000) inferred that an undifferentiated highly organic brown layer near the top of the core obtained from an oxbow lake indicated a period of increased eutrophication from 1840 to 1915 that likely followed the introduction of an invasive plant species and the construction of man-made dikes. Influence of human activities such as deforestation, dike-building, and eutrophication were also indicated by changes in organic content and sedimentation rates.

When employed in conjunction with other climate proxy data, flood history reconstruction can enable the determination the extent of combined effects of both climate and human activity on a river basin. Concerns regarding increased dry conditions in the Peace-Athabasca Delta (PAD) in northern British Columbia prompted a study of past flooding prior to the construction of a hydroelectric dam on the Peace River in 1968 (Wolfe et al. 2006). Existing instrumental records of river discharge covering only 9 years were insufficient to answer the question of whether periods of low flooding frequency were part of a natural cycle of variation for that region. Physical and geochemical analyses of laminated sediment records obtained from two oxbow lakes located in the PAD were used to reconstruct ice-jam flooding histories for the Peace River over the past 300 years. These results exhibited close agreement with historical records of past ice-jam floods, and confirmed that flooding frequency in the Peace River basin had varied considerably prior to 1968, indicating several 20 + year intervals of no major flooding before construction of the dam.

The relative roles of climate and river regulation in hydrological variability in the PAD were the subject of further investigation by Wolfe and others (2005). This study compared multi-proxy data (lake water isotope composition, organic carbon and nitrogen content, shifts in plant macrofossil and diatom assemblages) obtained by analysis of sediment cores from a lake near the Peace River with results of the previous ice-jam flood history reconstruction for that area and independent climate records (Wolfe et al.

2005). These results further substantiate the influence of climate in the long history of hydrological variability for the PAD; however, distinguishing between climatic and anthropogenic river regulation changes in hydroecology for the Peace River basin will require further investigation (Wolfe et al. 2005).

The objective of the study presented here is to identify signatures of Mohawk River flood events preserved within sediment of the Utica Marsh in central New York. Due to its location within the floodplain adjacent to the Mohawk River and Barge Canal and the fact that it has no other major inflow (Page, 1980) most sediment deposition in the Marsh results from overbank floods and wetland productivity (White and Rodbell, 2000). Low organic content (White and Rodbell, 2008) increases in magnetic susceptibility (Wolfe et al. 2006), decreased percentage of carbonate (Sant et al. 2004) and increased percentages of silt to sand-size grains (Sant et al. 2004; White and Rodbell, 2000) have been shown in studies of other locations to be indicative of hydrologic changes associated with overbank flooding (Walling et al. 1998). Dated sedimentological evidence of inferred flooding of the Mohawk River over the past 150-200 years was identified and compared with historical records of known flooding in the vicinity of the Utica Marsh to test the feasibility of reconstructing a sedimentological record of flooding history at this site.

Study Area

The Utica Marsh is a wetland area situated within the flood plain of the Mohawk River in Oneida County in central New York State (43º 6´ N, 75º 14´W). The bedrock of the area is comprised of granite, limestone, sandstone and shale overlain by glacial till left by the retreat of the Laurentide ice sheet over 10,000 years ago. These gravel deposits are covered by layers of silt and clay brought into the Utica Marsh by annual flooding of the Mohawk River (Williams, 1990). Mean temperatures for the area range between 11-21ºF in winter 60-80ºF during the summer. The area receives an average of 50 inches of rainfall and 70 inches of snowfall per year (Page, 1980).

Located north of the city of Utica, the Marsh area has been subjected to over 150 years of disturbance due to industrial and recreational activities. The area was mined for brick-making clay from the early 1900s through the 1940s, leaving pits which filled with water as the Marsh developed (Page, 1980). Slurry dredged from the nearby canal and Harbor was dumped in the area northwest of the Marsh between the Canal and the Mohawk River (Page, 1980). The construction of the Barge Canal in 1910, the Thruway in 1953 and the Horatio Arterial (Rt.12) in 1957 resulted in hydrologic changes which altered floodplain drainage patterns and caused the expansion of the Marsh from a narrow strip of land along the Mohawk River to its present 213 acres (Figure 2) (Page, 1980; Williams, 1990). The Marsh was bisected in 1835 by construction of an embankment for the present St. Lawrence Division CONRAIL train track which runs diagonally through the area from southeast to northwest, forming the North and South pools (Page, 1980). Increased wet conditions in the North Pool, possibly the result of poor drainage and percolation from the nearby Barge Canal, were evidenced by a change from wet meadow to emergent wetland vegetation since the construction of the Horatio Arterial in 1957 (Page, 1980). The South Pool retains water due to its deeper pools and obstruction to drainage caused by the Harry Roberts roadbed.

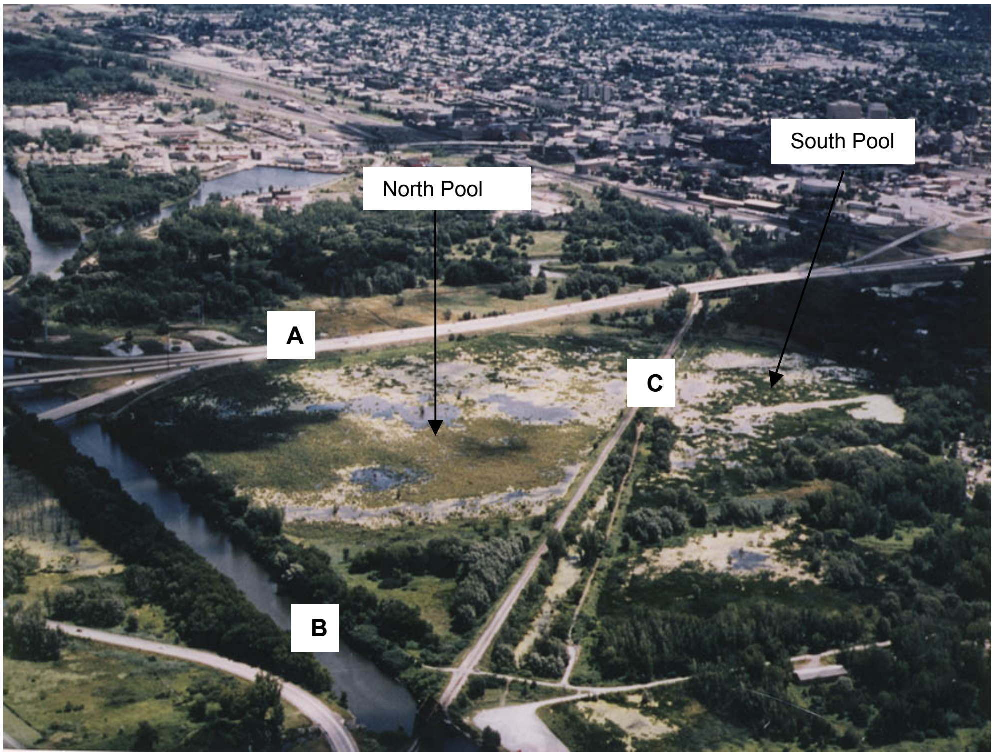

Figure 2: Aerial photo of the Utica Marsh and its location relative to the Horatio Arterial (**A**), Barge Canal (**B**) and Conrail track (**C**) (Hamilton College, 2009).

The Mohawk River is the largest tributary of the Hudson River, draining a total of 542 square miles (drainage basin size of 3456 sq mi) (Figure 3). From its origin in Lewis County the Mohawk River flows south to Rome, New York and southeast to Cohoes where it enters the Hudson River. Near Utica the Mohawk River receives discharge from two tributaries flowing from the south: Sauquoit Creek joins the river at Whitesboro and Oriskany Creek enters at Oriskany, New York.

Because of its location within the Mohawk River floodplain, the Utica Marsh is inundated yearly by floods resulting from snowmelt and rainfall in the late winter and

Figure 3: Map showing the location of Utica within the Mohawk River Basin in Central New York (Nystrom, 2008).

early spring, and thunderstorms and tropical storms in the summer and fall. The most significant cause of flooding on the Mohawk River is heavy winter or spring rain combined with snowmelt and ice jams. Eighty percent of high flow events (50,000 cfs or higher) occur between late winter and early spring (Gara and Garver, 2000). In severe floods, water from the Mohawk River has been observed to flow across the marsh and overtop the 10 ft canal banks, overflowing into the Canal. Although the river retreats rapidly following inundation, drainage of the Marsh area can take weeks (Page, 1980).

Flooding of the Mohawk River has impacted the surrounding area economically in a number of ways, particularly in structural and property damage, an increased the need for highway maintenance due to damage to roadbeds, and decreased land values caused by erosion of topsoil and sedimentation (Sauquoit Creek BWM, 1996). Tropical Storm Agnes brought 3.35 in of rainfall to the Utica area in 1972, triggering one of the area's largest floods. The flood caused an estimated $375,000 in damage, most of which was done to roads, sewers and catch basins ("Estimated Flood", 1972). An updated report to the Oneida County Board of Legislators suggests that the final cost was 'underestimated, with damages of a half-million dollars reported in the City of Rome alone (McCarthy, 1972).

Heavy rain throughout the summer of 2006, particularly in the month of June, resulted in over $20 million in damage to the Barge Canal system. Boating traffic through the state's four canals fell about 21% during the summer of 2006, and more than 80% of the canal system was closed during the month of July. In addition to loss of canal fees, economic impact was exacerbated by the loss of revenue to nearby restaurants and gas stations (Coin, 2006). The extent of damage to a region due to future flood events is a factor of the depth, velocity, rate of rise and duration of flood waters as well as the development of the floodplain and topography of the surrounding area (United States Army Corps of Engineers [USACE], 1974).

Methods

Core Collection and Preparation

Three sediment cores were collected along a 50 m transect located in an area of the Marsh north of the Conrail track, with BCA1 obtained from the most landward site, DOC from the middlemost site, and BCA5 from a site closest to the edge of the North Pool and nearest to the Mohawk River (Figure 4). The area was covered with shallow water varying in depth from a few centimeters at the landward site to over 0.5 m at the poolward site. Two of the cores (BCA1; BCA5; each 50 cm in length) were collected using a Russian peat borer (5.0 cm in internal diameter) (Jowsey, 1966). In each case surface vegetation and peat were moved aside in an effort to collect the samples at soil level. A third core (DOC), 36 cm in length**,** was collected using a polycarbonate mud-water interface corer (6.8 cm in internal diameter) in order to obtain a greater volume of recovered sediment, with the additional sediment being reserved for analysis in a separate study. The BCA1 and BCA5 cores were extruded in the field, sub-sampled at 1 cm increments and stored in individual plastic bags; the DOC core was extruded and sub-sampled in the lab and stored at 3˚C prior to laboratory analyses. The bottom 5 cm of DOC was accidentally lost during sub-sampling. Percent dry weight was calculated by weighing the wet samples, drying them at 60°C, and re-weighing. The dried samples were ground and split; 1-1.5 g subsamples were removed at every other centimeter and reserved for radiometric dating analysis. The remaining sediment for each interval was analyzed for changes in bulk density, organic content, magnetic susceptibility and grain size.

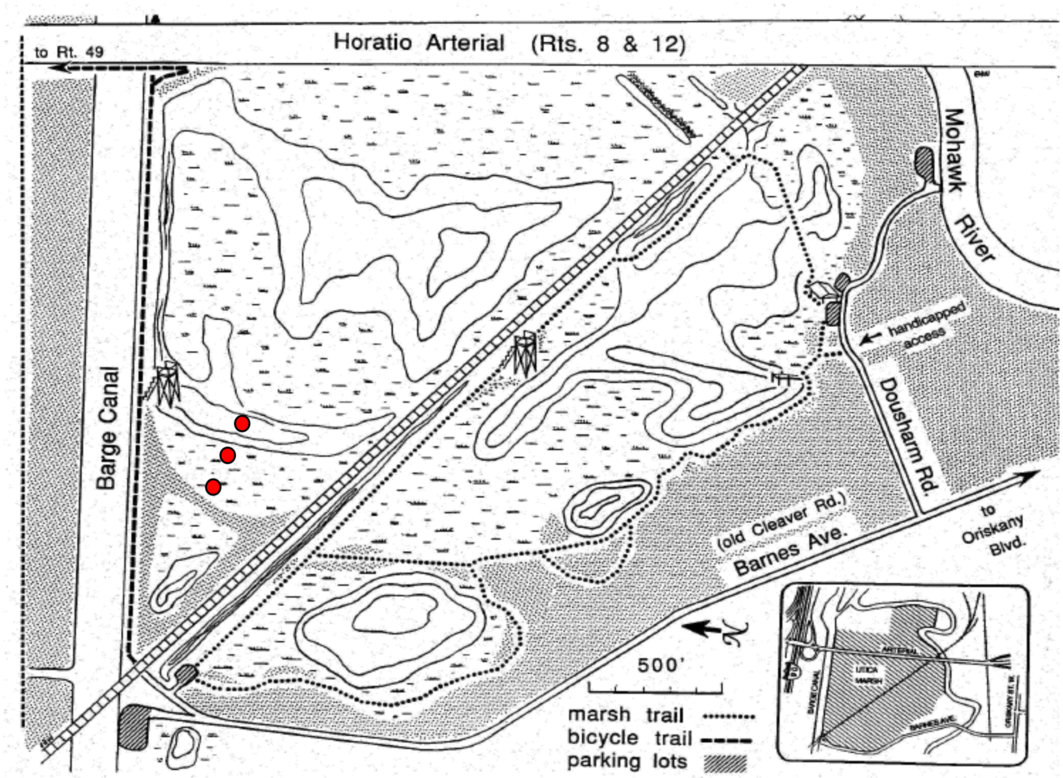

Figure 4: Map of the Utica Marsh showing approximate coring locations (BCA1 was obtained closest to the canal, DOC from the middlemost site and BCA5 from the site closest to the pool) (Hamilton College, 2009).

Chronology of Cores

Age-model determination of cores obtained from the Utica Marsh was carried out via analysis of ^{137}Cs and ^{210}Pb in 1-2 g samples of dried sediment sub-sampled from 1 cm intervals. The combined use of ^{137}Cs and ^{210}Pb is common, and concurrence between these two methods can yield accurate results in determining core chronology (Appleby, 2000; Craft and Casey, 2000). Both elements have a relatively quick rate of decay (half-life $\tau = 30.2$ yr for ^{137}Cs and $\tau = 22.3$ yr for ^{210}Pb) making them suitable for dating layers deposited within the last 100 years (Ritchie and McHenry, 1990; Collins et al., 2001).

Cesium-137 is an artificial radionuclide that first appeared in the environment in the late 1950s as fallout produced during atmospheric thermonuclear bomb testing. The analysis of ^{137}Cs should reveal a distinct peak in concentration which can be ascribed to 1963, the year of maximum atmospheric bomb testing (Ritchie and McHenry, 1990). The use of this peak as a time marker provides a means of estimating sedimentation rates over the past 30-35 years (Walling and He, 1998; Owens et al. 1999, Craft and Casey, 2000). A second smaller peak coincides with 1954, the year of initial fallout of ^{137}Cs; however, this peak is often diminished as a result of bioturbation and sediment mobilization and is rarely used in wetland studies (Craft and Casey, 2000). Additional ^{137}Cs fallout was also produced during the Chernobyl disaster in 1986, sometimes showing up as a small peak in sediments obtained from the Northern Hemisphere (Lima et al. 2005; Appleby, 2000).

There are two natural sources of ^{210}Pb in the environment: supported ^{210}Pb forms as a result of radioactive decay within the sediments and is assumed to be in equilibrium with its parent nuclide ^{226}Ra, while excess or unsupported ^{210}Pb is produced by atmospheric decay of ^{222}Rn, the gaseous daughter nuclide of ^{226}Ra. Unsupported ^{210}Pb binds to fine aerosol particles and settles to the ground as dry fallout or precipitation where it later washes into lakes and rivers and incorporated into the sediment record. Activity of $^{210}Pb_{unsupp}$ within a sediment profile is determined by subtracting the activity of $^{210}Pb_{supp}$ (assumed to be equivalent to activity of ^{226}Ra) from total ^{210}Pb activity.

Total ^{210}Pb activity, as well as activity of ^{137}Cs, can be measured directly by means of a technique called gamma ray spectroscopy. Unstable nuclei produced by the radioactive decay of ^{137}Cs and ^{210}Pb produce gamma ray energy in the form of photons.

This energy is captured by a sodium iodide (NaI) detector, converted into an electronic signal, and used to generate a gamma ray spectrum (a display of gamma intensity versus energy). Two dated historic events, nuclear bomb tests in 1963 and the Chernobyl disaster in 1986, typically provide distinct peaks in a gamma ray spectrum produced by ^{137}Cs activity (Collins et al., 2001). These markers together with sedimentation rates determined by regression from activity of unsupported ^{210}Pb can be used to date the sediment layers (Appleby and Oldfield, 1978).

Gamma ray spectroscopy was carried out on the sediment samples using a 3-inch NaI well detector (*St. Gobain*) with a tube-base digital multichannel amplifier (*Ortech DigiBase*). Activity of ^{137}Cs and ^{210}Pb was determined via their gamma emissions at 661 keV and 49 keV respectively. A blank sample was analyzed for 24 hours followed by a known weight of sample for 24 - 48 hours. The number of counts per second particular to each blank and sample was calculated, after which values for blanks were subtracted from values for the subsequently measured sample.

Dry Bulk Density Determination;

Each core was sectioned into 1 cm increments and dried at 60°C. The dry weight was used to determine the bulk density as follows:

$$\text{Bulk Density} = \text{dry weight of sample} / h (\pi r^2)$$

Bulk density is a measure of the weight per unit volume of a sediment sample. The volume of the sample is calculated as the volume of a cylinder with a height of 1in (length of the increment) and a radius equal to that of the particular corer used to collect the sample (3.4 cm for the polycarbonate mud water interface corer used to collect DOC and 2.5 cm for the Russian peat borer used to collect BCA1 and BCA5). Since only half of the sample was weighed for this analysis, the resulting volume (36.30 cm^3 for DOC; 19.27 cm^3 for BCA1 and BCA5) was divided by 2 to give the final volume of each sample (18.14 cm^3 for DOC and 9.81 cm^3 for BCA1 and BCA5).

Factors such as mineral composition, percent organic content, and grain size affect bulk density of a sediment sample by increasing or decreasing its porosity or space between particles. Bulk density increases with depth within a sediment sample due to compaction and dewatering and loss of organic matter over time. However, changes in bulk density superimposed on the long compaction trend can be interpreted as changes in the depositional environment (White and Rodbell, 2000). Increases in bulk density within a sediment record obtained from a floodplain could be interpreted as periods of drying due to drought or anthropogenic activities such as dredging or drawdown of water levels. Decreases in bulk density could represent episodes of inundation and saturation during a flood event (Allguire and Cahill, 2001).

Loss-on-Ignition Analysis (LOI)

The determination of the weight percent of organic carbon and inorganic carbon in the form of carbonate in sediment layers can be used to measure past productivity in the marsh, as well as provide information on processes that influence the cycling of carbon and other nutrients within a watershed (Wolfe et al. 2006). The organic carbon and inorganic carbonate content of the samples was estimated by loss on ignition analysis (LOI), a qualitative method based on differential thermal analysis (Dean, 1974; Santisteban et al. 2004). The index of the organic content of each core sub-sample was determined by the percent of weight lost after the sample had been dried at 60º C for 24 hours and ashed in a muffle furnace at 550 º C for four hours (to convert organic matter to CO_2). The sample was then ashed at 950 º C for two hours to drive off CO_2 and quantify the amount of carbonate (inorganic carbon) present in the sample (Dean, 1974). Organic matter and total carbonate content were expressed as percent of the dry sediment weight.

Determination of carbon content by means of loss-on-ignition analysis is used in reconstruction of flood history and other paleoclimatic studies. However, comparison with geochemical and multi-proxy evidence is necessary in order to distinguish between organic material produced by autochthonous processes within a floodplain and allochthonous organic material supplied by periodic floods (Wolfe et al. 2005). Decreases in carbon content accompanied by increases in magnetic susceptibility within dark-colored laminae of an oxbow lake were interpreted as of past flood events. High energy conditions associated with flood activity can result in dilution of organic matter with inorganic (fluvial) sediment, as well as decreased productivity due to increased turbidity (Wolfe et al. 2006; Thom et al, 2001). However, low organic content in sediments of a perched basin lake can also interpreted as resulting from low preservation of organic matter during dry periods (Wolfe et al. 2005).

Magnetic Susceptibility

Magnetic susceptibility measures the ability of a material to be magnetized and is related to changes in composition, concentration and particle size of ferrimagnetic minerals (ie. magnetite) in a sediment sample (del Soccorro and Ortega-Guerrero, 1998).

Magnetic measurements have been used in the study of lake sediments since 1975 (Thompson, 1975). Since specific minerals exhibit particular magnetic behaviors, magnetic measurements can provide evidence relating to the source of sediments, such as detrital versus autogenic (Walling et al. 1979) as well as the nature of depositional processes (Wolfe et al.2006). Variation in magnetic measurements can reflect changes in conditions in past depositional environments. In this way, magnetic susceptibility changes are proxies of past environmental conditions (Geiss, 1999). Peaks in magnetic susceptibility measurements have also been used to correlate chronology of sediment cores in reconstruction studies (Appleby et al. 1985, Ruggiero et al. 2000).

Magnetic susceptibility was measured on dried samples of Utica Marsh sediment at each 1 cm interval for all three Utica Marsh cores using a Bartington *MS2* single sample dual frequency sensor. The average magnetic susceptibility value for each sample was divided by the sample dry weight to obtain the mass specific magnetic susceptibility (χ) and expressed as $10^{-6}cm^3/g$ units. Similarly, the average magnetic susceptibility value for each sample was divided by the sample volume to obtain the volume specific magnetic susceptibility (κ) and expressed in $x10^{-5}$ SI (standard international) units (Dearing, 1999).

Grain Size Analysis

Grain size analysis of Utica Marsh sediment was determined by means of a laser diffraction particle size analyzer (Model: Malvern Mastersizer 2000). Subsamples were analyzed at 1 cm intervals following removal of organic matter by hydrogen peroxide treatment, addition of sodium hexametaphosphate $(NaPO_3)_6$ as a dispersing agent, and sonication. Laser diffraction operates on the principle that the angle at which a particle diffracts light increases as particle size decreases. The resulting particle size spectra are used to calculate percentages of clay, silt, sand, median grain size and population standard deviation (sorting) of grain sizes within a sediment sample.

Grain size characteristics within a floodplain profile can vary in response to factors affecting sediment transport and depositional processes. Sediment source composition, flood magnitude and flow velocity, particle aggregation, channel configuration and floodplain topography can influence grain size composition of overbank floodplain deposits (Lecce and Pavlowsky, 2004). Irregularities in floodplain topography create spatial and temporal variations in water depth, flow velocities, and inundation times (Lecce and Pavlowsky; Walling and He, 1998), all of which can affect particle-size distribution and sedimentation rates over a floodplain. Thus, grain size analysis is important in the study of floodplain development and morphology (Walling and He, 1998). Because a floodplain forms primarily as a result of fine-grained suspended sediment transported and deposited during overbank flood events, it becomes a sink for nutrients and pollutants which have a tendency to adhere to fine-grained particles (Walling et al. 1998; Walling and He, 1998). Understanding grain size distribution within floodplain sediments is thus also important in the study of factors affecting the storage and re-mobilization of contaminants within the floodplain (Winter et al, 2001; Walling and He, 1998; Lecce and Pavlowsky, 2004).

Changes in grain size relative to background within a sediment profile can be indicative of high energy fluvial processes associated with floods. Stratigraphic increases in grain size accompanied by increased quartz and feldspar content and higher magnetic susceptibility values within sediments obtained from an oxbow lake were interpreted by Wolfe and others (2006), as evidence of high energy depositional environments associated with flood events. Huang and others (2007) interpreted peaks in percentages of sand-sized grain fractions within loess-soil sequences as overbank flood deposits. Sant and others (2004) interpreted increases in percentages of >149 μm particle size fractions within unstratified floodplain sediments along the Mahi River as flood deposits associated with strong monsoon events. Because of their correlation with oscillations between weak and strong monsoon periods, these particle size variations are proxies of climate change during the period extending from 30 ka to the onset of the Holocene. Stratigraphic changes in grain size within oxbow lake sediments are also indicative of sediment provenance, enabling White and Rodbell (2000) to differentiate between detrital sediments deposited during erosional events and suspended sediment deposited during overbank floods throughout the development of the lake. Thus, grain size analysis of overbank floodplain sediments can yield evidence useful in the reconstruction of flooding history for a river basin.

Results

Subsamples from each of the three cores were obtained for bulk density, magnetic susceptibility, organic carbon and carbonate content, and grain size. The results of these analyses versus bottom depth for each core are shown in Figures 5-7 and core-to-core comparisons are shown in Figures 8-14 below.

Core Characteristics

BCA5

BCA5, 50 cm in length, is the core obtained from the site closest to the pool and the Mohawk River. The results of the analyses carried out on BCA5 are presented in Figure 5. Bulk density (a) ranges from a minimum of 0.03 ± 0.3 g/cm^3 at 1 cm to a maximum of 1.02 ± 0.3 g/cm^3 at 31 cm, showing an increasing trend with core depth. Mean bulk density for BCA5 is 0.6 g/cm^3. Values for percent carbonate and percent organics for the first 5 cm of the core were not determined due to loss of sub-samples during laboratory processing. Percent organic matter (c) ranges from a minimum of 2.0 % ± 0.4 at 30 cm to a maximum of 3.8% ± 0.4 at 7 cm, showing little variation and no significant trend between 12 and 44 cm. Mean percent organic matter for BCA5 is 2.6%. Percent carbonate (d) varies throughout the length of the core, but generally increases with depth to a maximum of 2.1% ± 0.3 at 28 cm, after which it displays a decreasing trend reaching a minimum of 0.8% ± 0.3 at the core bottom (44 cm). The mean value for percent carbonate in BCA5 is 1.4%. Percent clay (e) ranges between a minimum of 25.5% ± 2.6 at 4 cm to a maximum of 40.9% ± 2.6 at 44 cm, increasing sharply to a peak from 6 to 9 cm followed by a sharp decrease at 11 cm, after which percent clay values ranges between 35.0 and 40.0% with a mean value at 38.0%. Percent silt (f) displays higher values with a similar peak at 6 cm, followed by a sharp decrease to a minimum of 53.6% ± 1.3 at 11 cm, after which it shows only a slight overall increase with depth from 12 to 44 cm. However, percent silt exhibits numerous peaks from 15 cm to the bottom of the core, with particularly strong peaks at 22 and 27 cm, increasing to a maximum of 59.2% ± 1.3 at 38 cm. Most values for percent silt fall between 55.0 and 60.0%, with the mean value at 57.3%. The highest values for percent sand occur within the upper 10 cm of the core, ranging from a maximum of 20.9% ± 3.5 at 11 cm to a minimum of 0.7% ± 3.5 at 6 cm. Most values for percent sand (g) are less than 5.0% for the rest of the core, while the mean value is 4.74%. Insufficient sample size prevented grain size analysis of the first 4 cm of BCA5. Magnetic susceptibility (b) decreases from a maximum of 85.1 ± 11.5 $x10^{-6}cm^3/g$ at 1 cm to a minimum of 16.8 ± 11.5 $x10^{-6}cm^3/g$ at 4 cm, after which it shows little variation and only a slight decreasing trend to the bottom of the core. The mean value for magnetic susceptibility in BCA5 is 25.6 $x10^{-6}cm^3/g$.

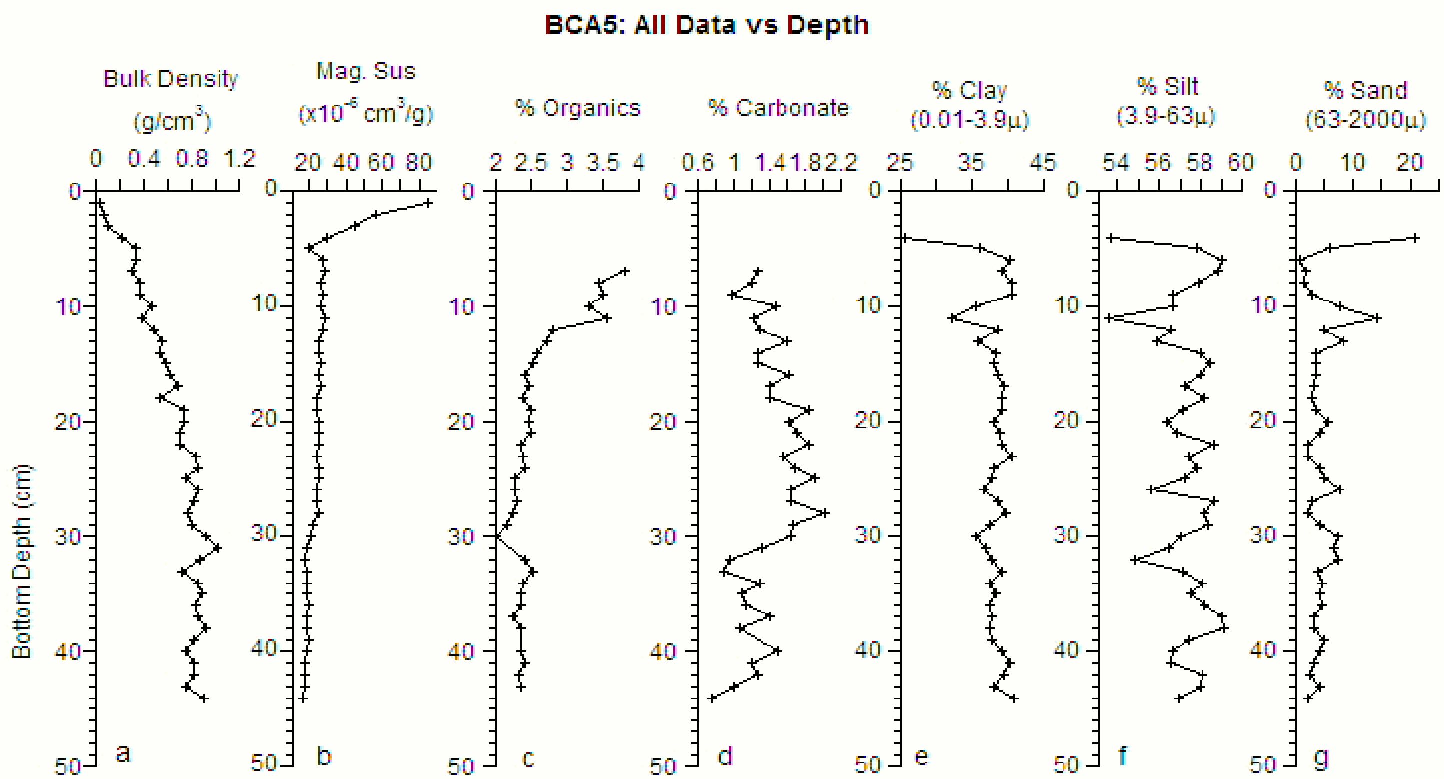

Figure 5: BCA5 data plotted versus depth.

DOC

The DOC: 50 cm core was obtained from a location midway between the shore and the North Pool. The results of the analyses carried out on DOC are presented in Figure 6. Bulk density (a) exhibits an overall increasing trend with depth, ranging from a minimum of 0.1 ± 0.3 g/cm^3 to a maximum of 1.1 ± 0.3 g/cm^3 at a depth of 14 cm. Most bulk density values are less than 1.0 g/cm^3; mean bulk density for DOC is 0.6 g/cm^3. Magnetic susceptibility (b) shows little variation with increasing depth, exhibiting a weakly-increasing tend to a maximum of 17.3 ± 3.3 $x10^{-6}cm^3/g$ at 22 cm, followed by a weakly-decreasing trend to a minimum of 6.6 ± 3.3 $x10^{-6}cm^3/g$ at 42 cm. The mean value for magnetic susceptibility is 12.4 $x10^{-6}cm^3/g$ for DOC. Percent organic matter (c) decreases from a maximum of 8.8% ± 2.0 at 1 cm to a minimum of 2.3% ± 2.0 at 23 cm, after which it increases with depth for the remainder of the core.

The mean value for percent organic matter for DOC is 4.0%. Percent carbonate (d) follows an overall weakly decreasing trend from a maximum of 2.7% ± 0.4 at 9 cm to minimum of 1.1% ± 0.4 at 39 cm, with peaks at 17, 23, 27 and 32 cm. Mean percent carbonate is 1.9% for DOC. Percent clay (e) ranges from a minimum of 22.0% ± 6.5 at 3 cm to a maximum of 45.1% ± 6.5 at 36 cm, exhibiting an overall increasing trend with increasing core depth. The mean value for percent clay is 36.5% for DOC. Percent silt (f) also increases for the first 14 cm of the core, after which it follows a weakly decreasing trend, ranging from a minimum of 43.7% ± 3.9 at 3 cm to a maximum of 59.6% ± 3.9 at 14 cm. Except for a trough between 3 and 7 cm, percent (g) sand decreases overall from a maximum of 34.3% ± 9.7 at 3 cm to a minimum of 0.3% ± 9.7 at 33 cm. The mean value for percent sand is 9.12% for DOC.

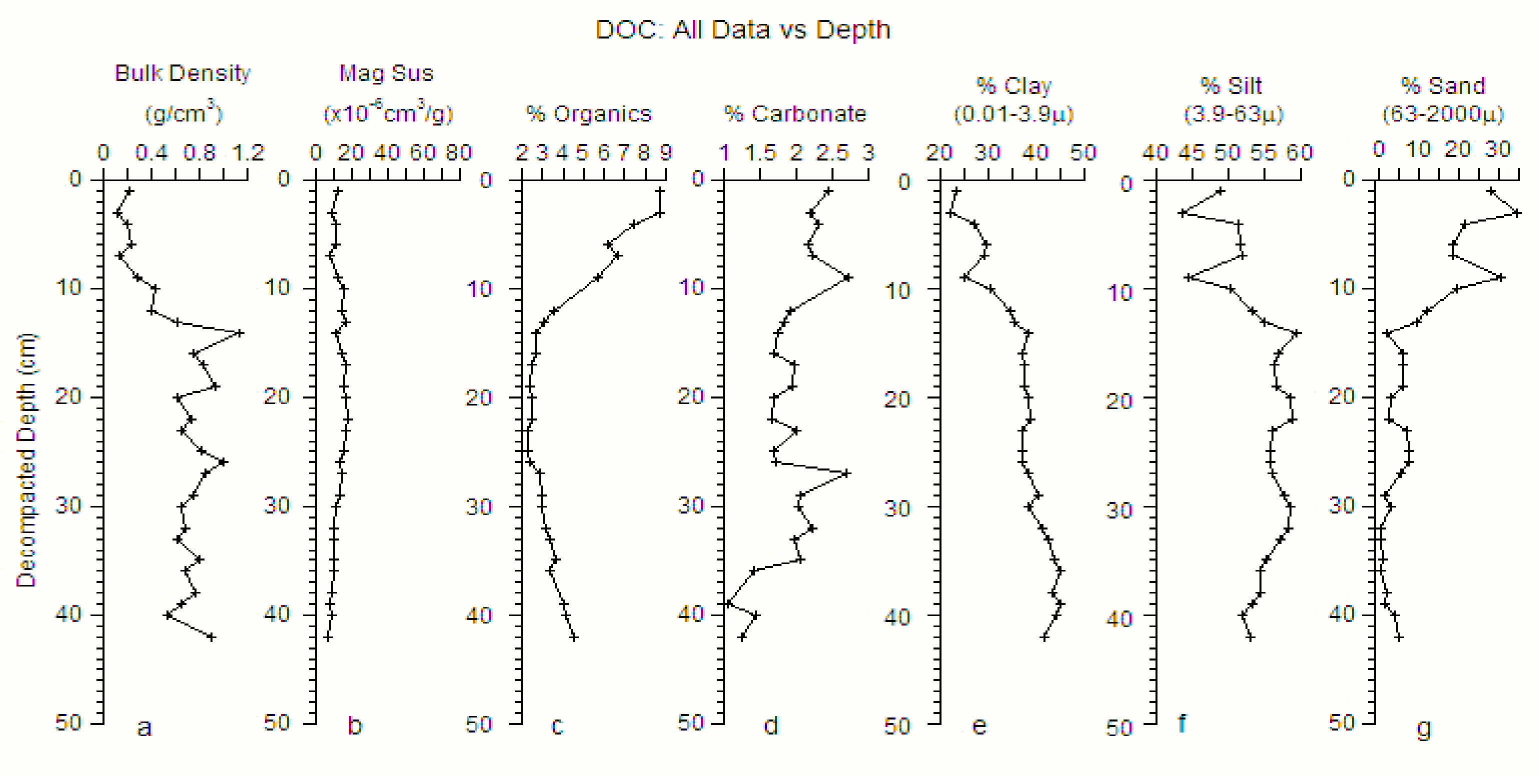

Figure 6: DOC core data plotted versus decompacted depth.

BCA1

BCA1, 50 cm in length, is the core obtained closest to the shore and farthest from the Mohawk River. The results of the analyses carried out on BCA1 are presented in Figure 7. Bulk density (a) in BCA1 increases from a minimum of 0.1 ± 0.1 g/cm^3 at 2 cm to a maximum of 0.6 ± 0.1 g/cm^3 at 27 cm. It exhibits a weakly-decreasing tend to 43 cm, after which it increases for the remainder of the core. Mean bulk density for BCA1 is 0.3 g/cm^3. Magnetic susceptibility (b) varies considerably in the upper 10 cm of the core, increasing from a minimum of 13.1 ± 13.6 x10^{-6}cm^3/g at 2 cm to maximum of 84.4 ± 13.6 x10^{-6}cm^3/g at 6 cm. Following a sharp decrease between 6 and 7 cm, magnetic susceptibility (b) exhibits a decreasing trend with most values falling between 10.0 and 20.0 x10^{-6}cm^3/g. The mean value for magnetic susceptibility for BCA1 is 24.9 x10^{-6}cm^3/g. Percent organic matter (c) increases to a maximum of 7.4% ± 1.4 at 5 cm and decreases to a minimum of 2.3% ± 1.4 at 22 cm. Values for percent organic matter remain at less than 25.0% until 30 cm, than increases overall for the remainder of the core. The mean value for percent organic matter is 3.9% for BCA1. Percent carbonate (d) shows considerable variation over a weakly decreasing trend with depth, ranging from a minimum of 1.8% at 33 cm to maximum of 4.2% at 39 cm. Percent clay (e) ranges from a minimum of 21.5% ± 0.4 at 2 cm to a maximum of 51.9% ± 0.4 at 41cm, showing a general increase with depth with some minor peaks. The mean value for percent clay is 40.5% for BCA1. Following a trough between 1 and 6 cm, percent silt (f) exhibits a weakly decreasing trend from 7 to 30 cm, where it decreases from a maximum of 59.1% ± 4.5 to minimum of 41.7% ± 4.5 at 42 cm then increases over the last 8 cm of the core. The mean value for percent silt is 52.9% for BCA1. Percent sand (g) ranges from a maximum of 27.2% ± 6.3 at 4 cm to a minimum of 0.5% ± 6.3 at 20 cm, displaying a weakly decreasing tend with considerable variation for the length of the core. The mean value for percent sand is 6.7% for BCA1.

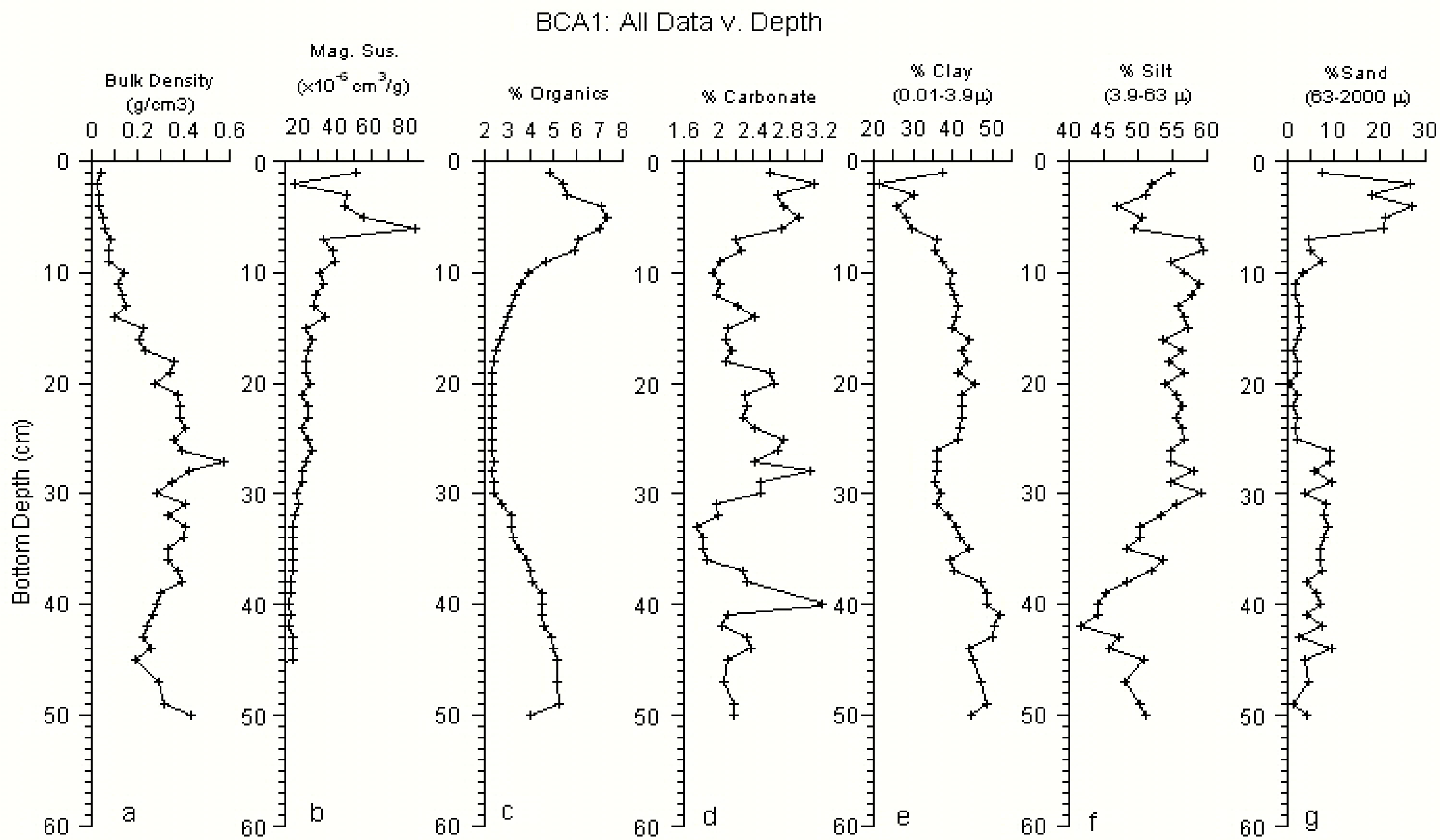

Figure 7: BCA1 core data plotted versus depth.

Core-to-Core Comparisons

Values for bulk density are lowest near the sediment surface and increase with depth in all three cores (Figure 8). Low values for bulk density in the upper level (0- 15 cm) coincide with increased percentages of organic matter within the same depth interval for all 3 cores. Values for percent organic matter are lowest in BCA5 (maximum of 3.8 ± 0.4% at 6 cm) (Figure 9). The highest values for magnetic susceptibility were observed in BCA1 and BCA5, with most values falling between 18.0 x 10^{-6} cm^3/g and 90.0 x 10^{-6} cm^3/g in the upper 10 cm (Figure 10). Although values for magnetic susceptibility are lower overall (< 18.0 x$10^{-6}cm^3/g$) for DOC, it exhibited highest amount of variability in magnetic susceptibility below 14 cm. Both BCA1 and DOC exhibit peaks in magnetic susceptibility at both 7-9 and 12-15 cm. Relatively little variation in magnetic susceptibility is noted in BCA5 below 5 cm. Bulk density values increase with depth overall below 10 cm for all three cores, while values for magnetic susceptibility tend to decrease with depth. Percent carbonate shows considerable variation in all three cores (Figure 11).

Grain size analysis revealed a trend of increased percentages of clay-sized particles with increasing depth except for a decrease near the sediment surface, with the sharpest decrease noted in BCA1 at 0-5 cm (Figure 12). A similar trend is noted for percentages of silt-sized particles in all cores, with a decrease noted in the upper 0-5 cm (Figure 13). Decreases in percentages of clay-sized particles tend to be accompanied by increases overall in both silt and sand percentages. Clear peaks in percentages of clay-sized particles correspond to decreases in silt-sized percentages within the 0-20 cm interval in all three cores. However, all three cores (most notably BCA1 and DOC) exhibit several clear peaks in sand-sized percentages which coincide with sharp decreases in silt-sized percentages within the same interval (Figure 14).

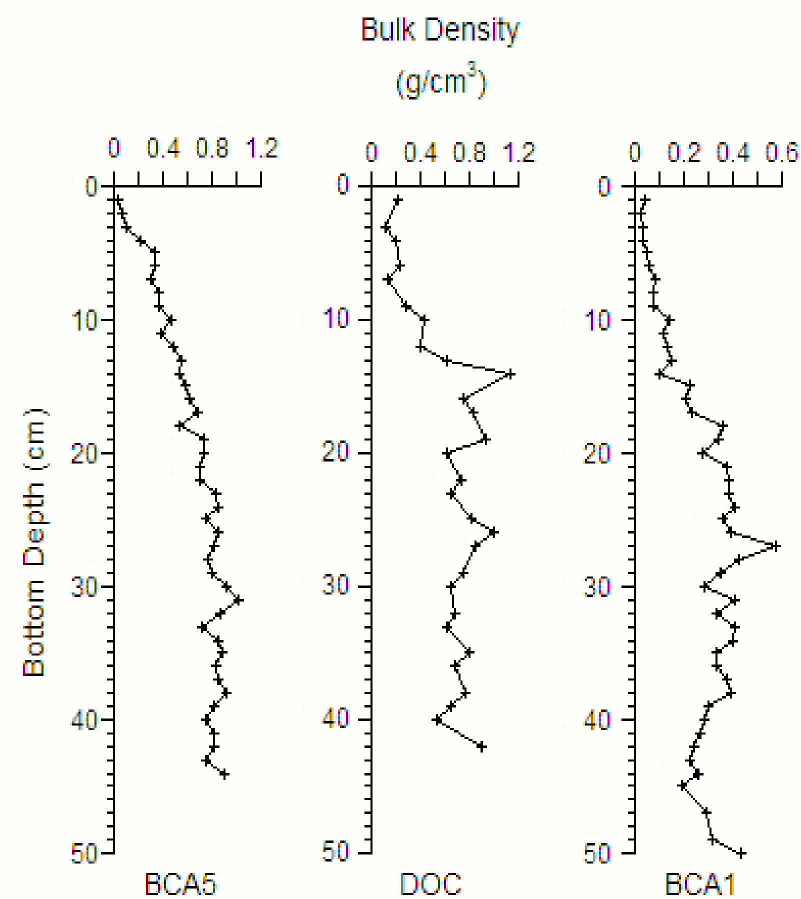

Figure 8: Bulk density versus depth (all cores).

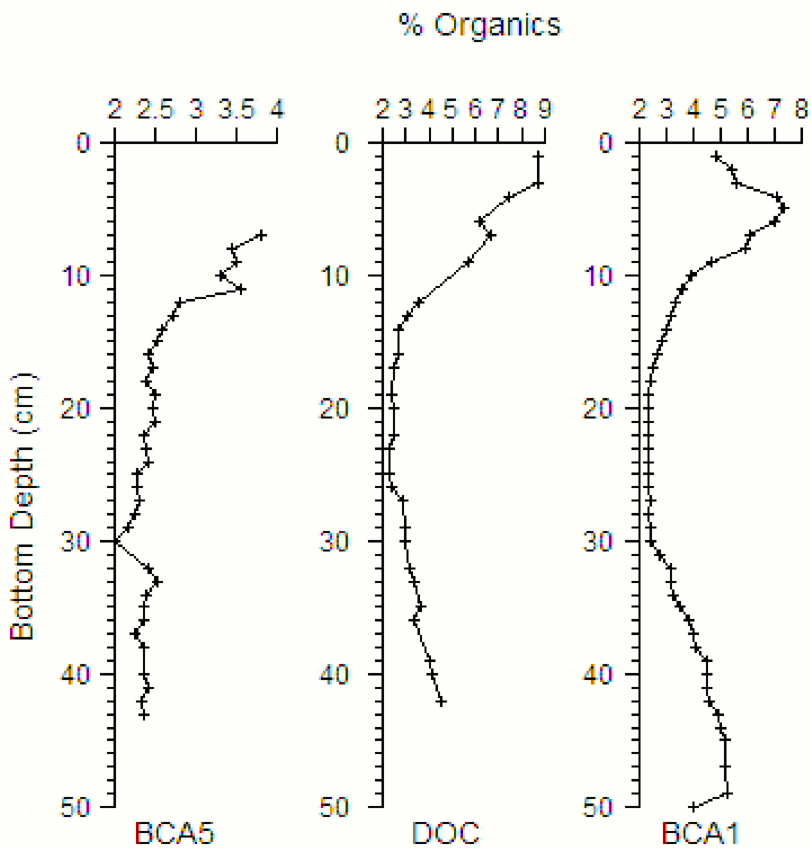

Figure 9: Percent organics versus depth (all cores).

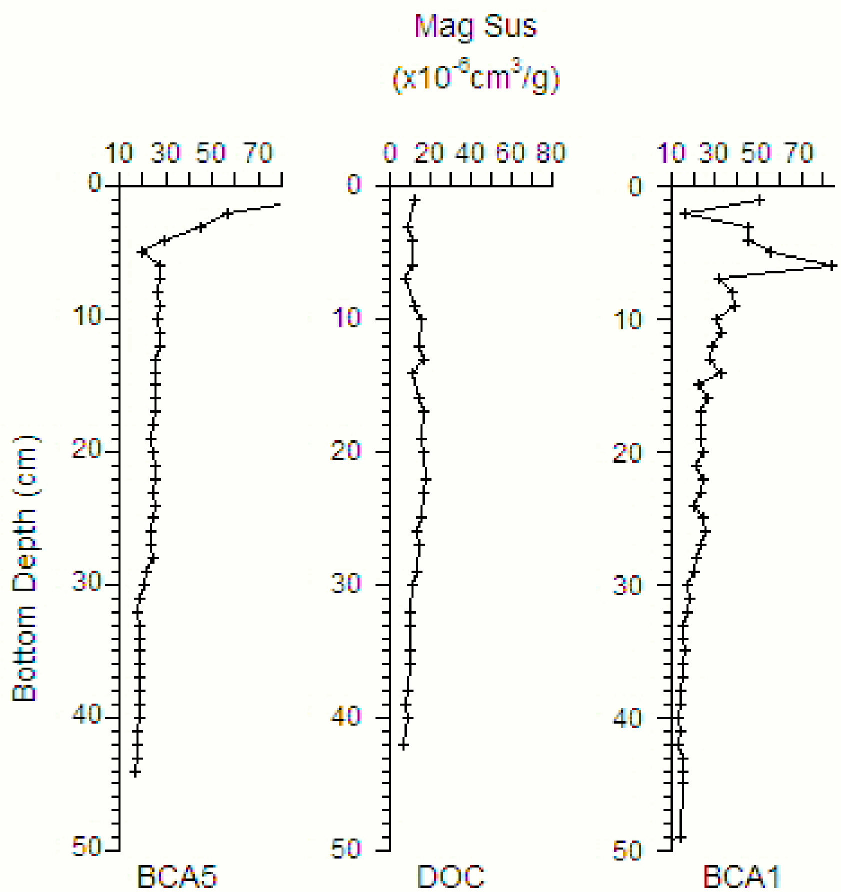

Figure 10: Magnetic susceptibility versus depth (all cores).

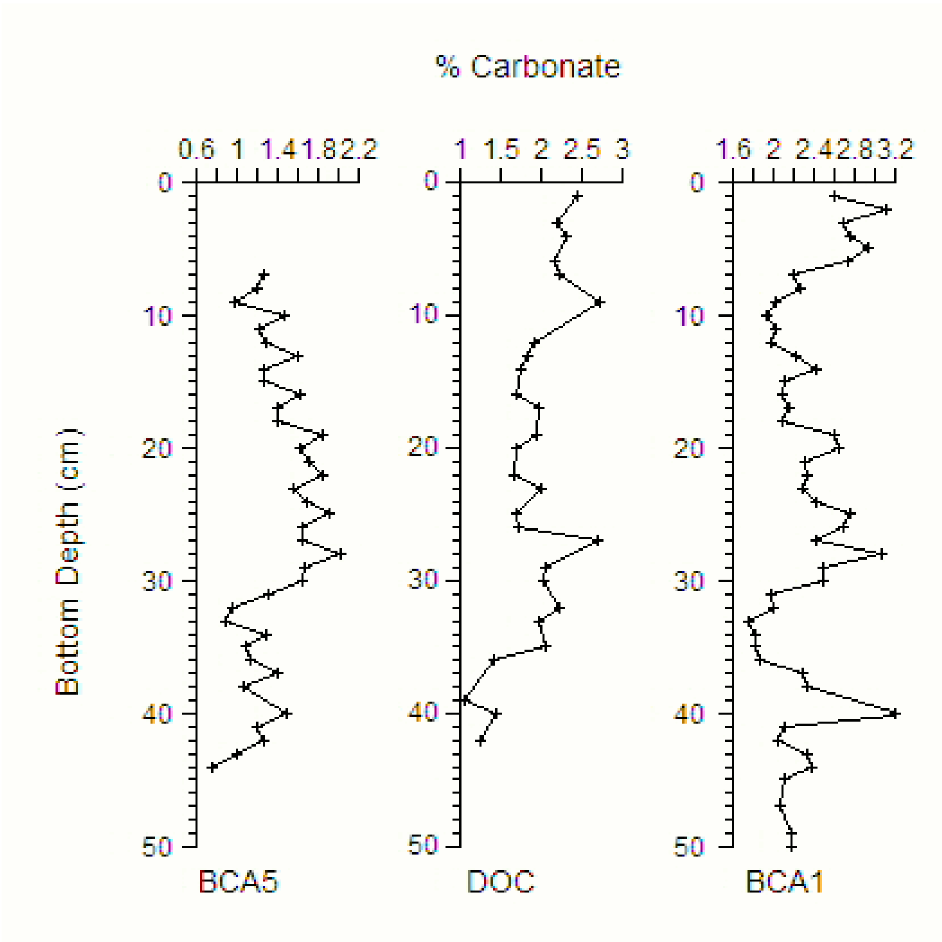

Figure 11: Percent carbonate versus depth (all cores).

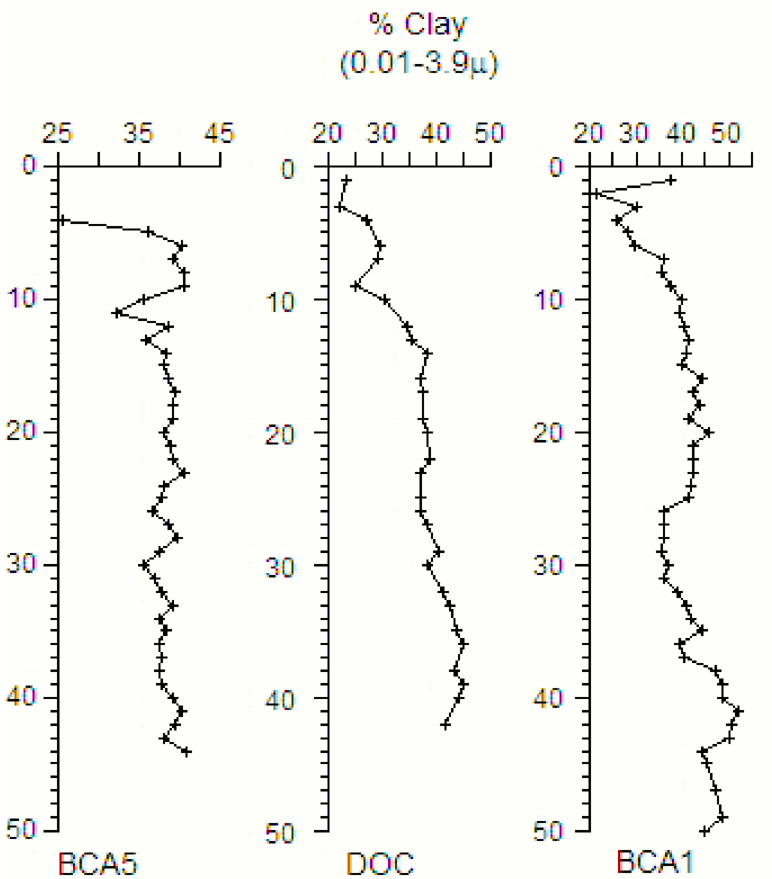

Figure 12: Percent clay versus depth (all cores).

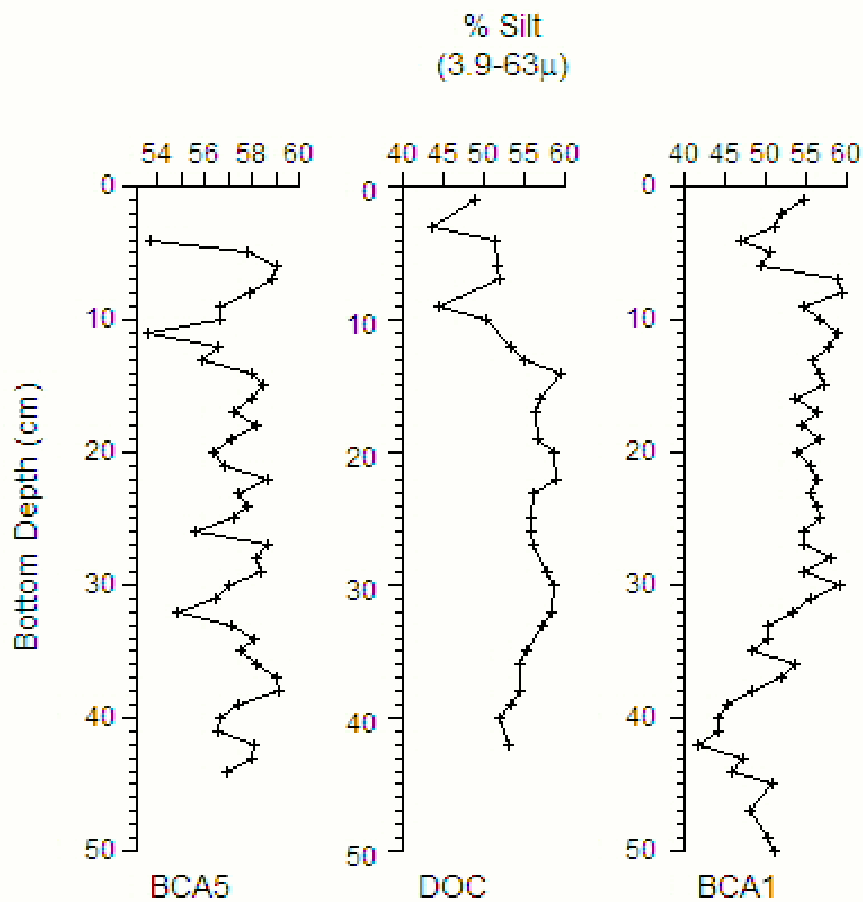

Figure 13: Percent silt versus depth (all cores).

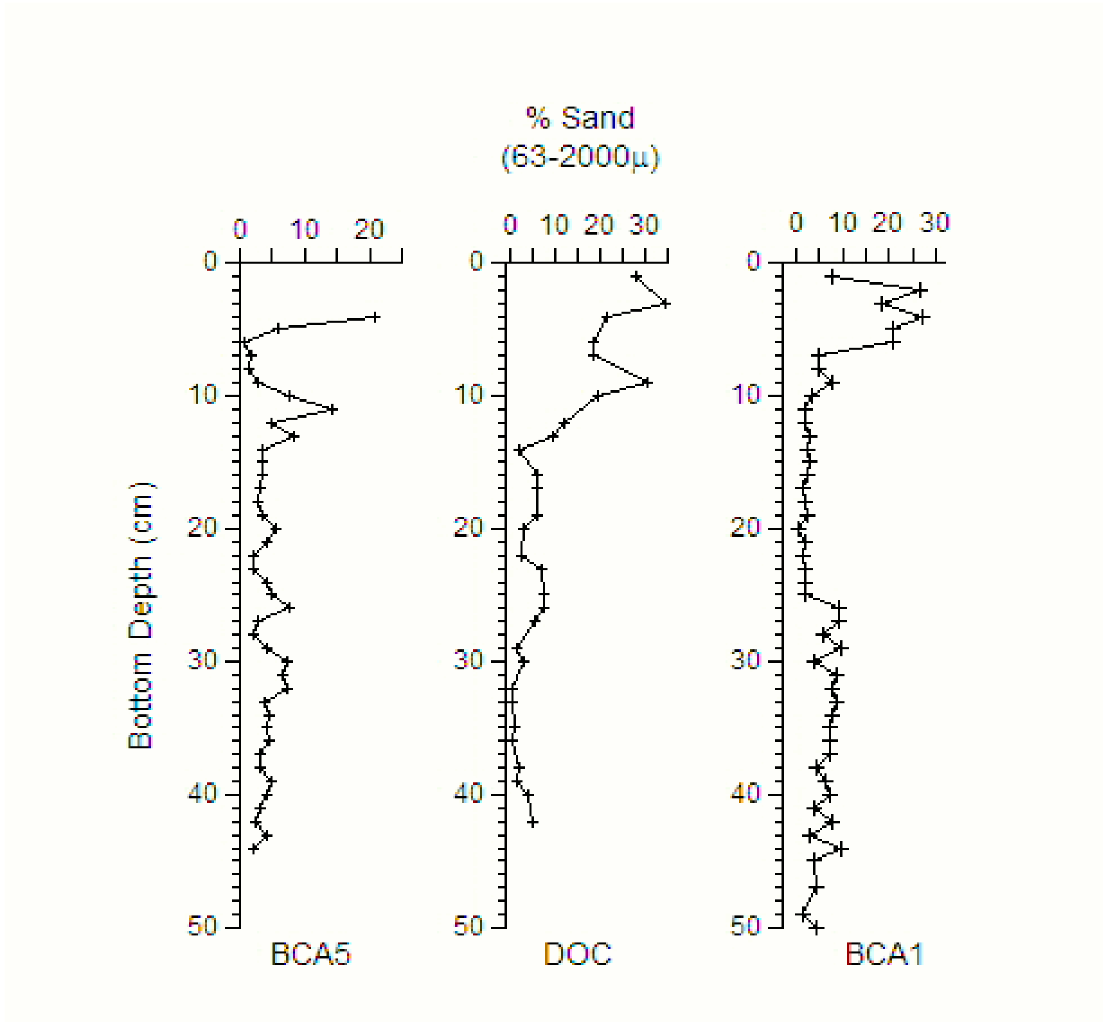

Figure 14: Percent sand versus depth (all cores).

Radiogenic Isotopes

Laboratory analyses carried out on the three sediment cores (BCA5; DOC; and BCA1) obtained from the Utica marsh included the use of radioactive isotopes ^{210}Pb and ^{137}Cs to establish core chronologies and determine average sedimentation rates. Results of ^{210}Pb data did not show an exponential decay with depth in any of the three cores (Figure 15). Peaks in cesium-137 are apparent at 14 cm depth in BCA1 and 7 cm depth in DOC. Two peaks (both ~ 0.009 cts/g/s) can be identified in BCA5 at 4 cm and 11 cm (Figure 16).

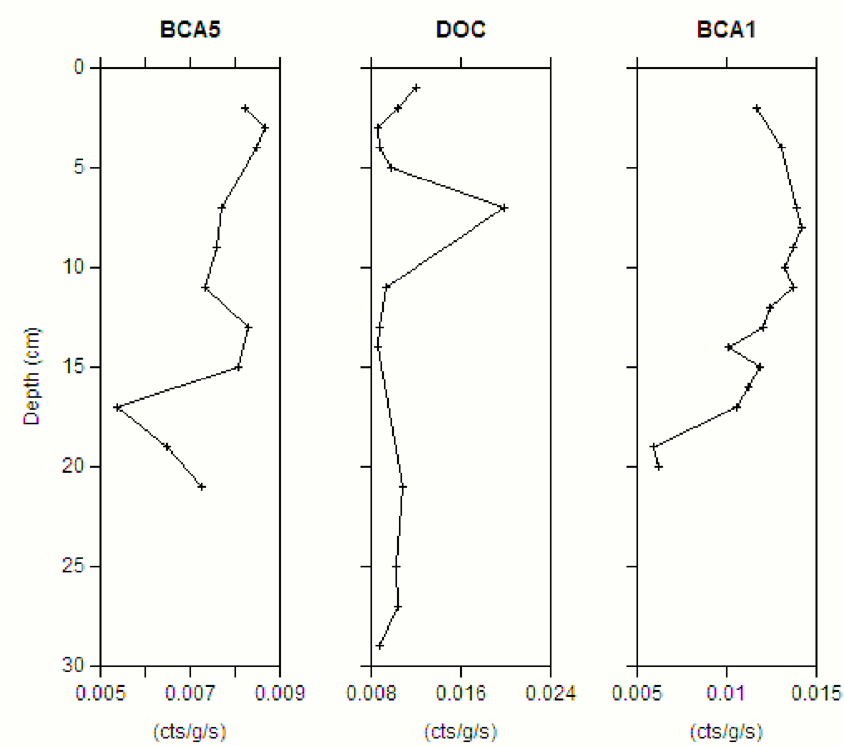

Figure 15: Activity of ^{210}Pb versus depth (all cores). Lead-210 values did not show the expected exponential increase with depth, possibly due to post-depositional mixing of sediment by either bioturbation or physical processes.

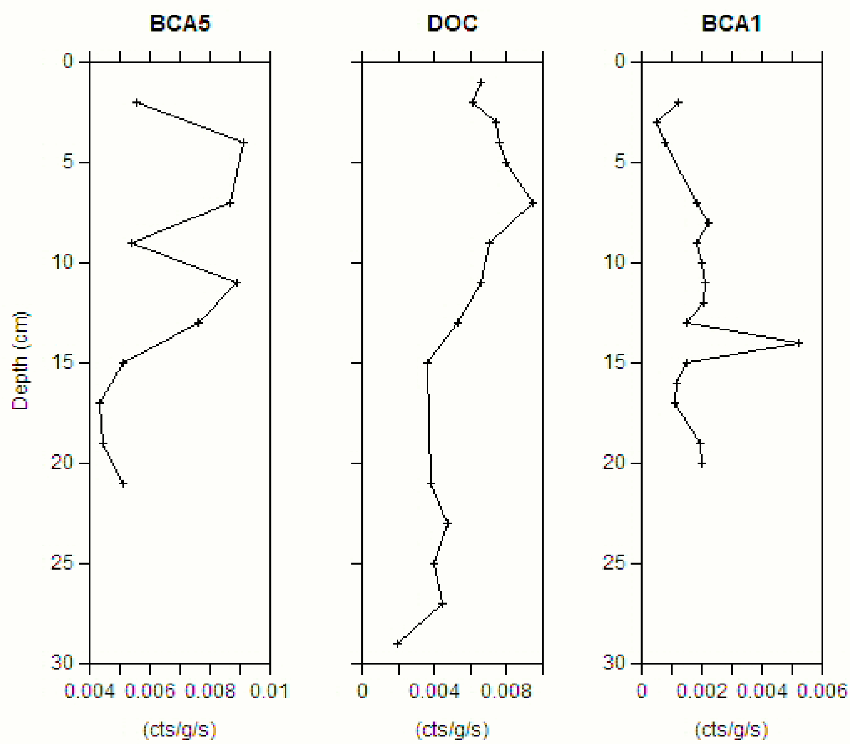

Figure 16: Activity of cesium-137 versus depth (all cores). Peaks at 14 cm depth in BCA1, 11 cm in BCA5 and 7 cm depth in DOC can be interpreted as resulting from thermonuclear bomb testing in 1964. A second peak at 4 cm depth in BCA5 may represent the Chernobyl nuclear disaster in 1986.

Discussion

The establishment of an age model was complicated by the fact that ^{210}Pb values did not show the expected exponential decrease with increasing depth (Figure 15). Three reasons could account for this: 1) Increased rates of sediment accretion over the last century due to increased land use may have diluted the input of atmospherically derived ^{210}Pb. 2) The excavation of clay that occurred within the Marsh during the early 1900s through the 1940s may have caused an influx of sediment into the study area, disturbing the pre-existing sediment sequence and resulting in the type of dilution effect described above (Page, 1980; Williams, 1990). 3) Post-depositional mixing of sediment layers may have occurred as a result of either bioturbation or physical processes (Brenner et al. 2001). Because of its location within the floodplain, Utica Marsh sediment would be subject to re-mobilization and mixing during Mohawk River flood events (Walling and He, 1998).

Activity of cesium-137 also showed little variation with depth, resulting in only a slight peak that could correspond to periods of maximum fallout in 1963 (Figure 16). Because of its strong tendency to bind to clay-sized particles, cesium-137 is also subject to post-depositional mobility and mixing by flood waters (Craft and Casey, 2000). Bioturbation and uptake by plants can also cause redistribution of cesium-137 in marsh sediments (Brenner et al, 2001).

Dating of the cores and determination of average sedimentation rates was based on linear interpolation between the cesium-137 peak and an assumed core top age of zero, with extrapolation of the same sedimentation rate to the core base (Figure 17).

Average linear sedimentation rates were estimated at 0.186 cm/yr for BCA5, 0.141 cm/yr for DOC and 0.079 cm/yr for BCA1. These sedimentation rates were applied to the full

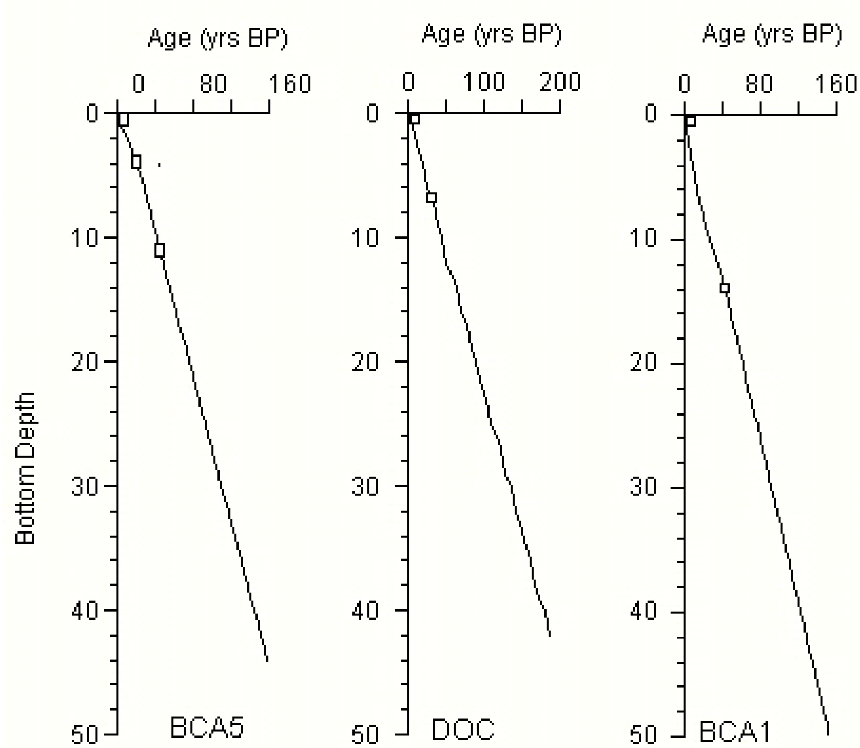

Figure 17: The calculated age for each core is plotted versus depth to represent sedimentation rates for each core. Due to problems with radiometric dating resulting from post-depositional mixing of the sediment, sedimentation rates are estimated based on linear interpolation between the cesium-137 peak and an assumed core top age of zero, then linear extrapolation of the sedimentation rate to the core base.

length of the stratigraphic records to establish core chronologies. On this basis, BCA5 spans approximately 180 yrs BP to 1828 AD and BCA5 spans approximately 150 yrs to 1851 AD.

The DOC core was collected by means of a poly-carbonate mud-water interface (vertical push) corer which resulted in compaction of the sediment and a raw compacted depth of 36 cm. Therefore, determination of sedimentation rates and resulting core chronology for the DOC record were based on a decompacted depth of 50 cm, the total depth of core barrel penetration, yielding an average sedimentation rate of 0.141 cm/yr. Based on application of this sedimentation rate, the DOC core spans approximately 220 yrs to 1785 AD. The age in years of all three cores extends from a core top age of 2005, the year of core collection (Figure 17).

A peak in magnetic susceptibility values observed within the upper section (0-10 cm) of each core (Figure 10) could be indicative of a recent flood event. Wolfe and others (2006) interpreted increases in magnetic susceptibility accompanied by decreases in carbon content within dark-colored laminae of an oxbow lake as flood events. Peaks in magnetic susceptibility within the sediment layers coincided with historic records of high water events (Wolfe et al 2006). However, magnetic susceptibility values show little variation below 10 cm for BCA1 and BCA5, possibly due to remixing and dilution of the magnetic mineral input during earlier overbank flood events. Huang and others (2007) attributed higher magnetic susceptibility values in the soil layers to pedogenic (soil building) processes; however, decreased magnetic susceptibility measurements observed within the soil layers were attributed to the addition of alluvial sediment during overbank flood events.

The peak in magnetic susceptibility observed in the top layer of each core could also be attributed to increased inputs of magnetic minerals resulting from land use and erosion. Influxes of magnetic-rich minerals from the surrounding drainage basin produce high magnetic susceptibility values which are interpreted as floods, erosion, or increased precipitation from which can be inferred changes in climate and human activity (Kirby et al. 2004;Wolfe et al 2006). It could also be indicative of an influx of heavy metals in recent years due to pollution and automobile emissions, as the sediment interval corresponds to the time period following the construction of the Horatio Arterial (Rt. 12) in 1957 (Figures 18-20) (Ramessur and Ramjeawon, 2002; Whiteley and Murray, 2005).

The lowest bulk density values are observed within the upper 20 cm of each core and are accompanied by an increase in grain size (Figures 5-7). Lower values for bulk density are also accompanied by higher values in organic matter in the upper 10 cm of each core (Figures 5-7). An increase in percent organic matter causes a reduction in the bulk density of sediment by increasing the tendency of sediment particles to aggregate, resulting in increased porosity. A higher percentage of organic matter could be the result of increasing plant biomass and corresponding increase in primary productivity over the last 50 years resulting from the development of wetland conditions in the floodplain (ie. the development of the Utica Marsh) and resulting expanse of emergent vegetation (Page, 1980). Herrick and Wolfe (2005) determined that artificially diked wetlands exhibit significantly higher levels of organic matter than undiked wetlands. The construction of the Canal and Arterial may have had the effect of diking the Marsh, increasing its ability to act as a sink for nutrients such as organic carbon. The time period represented by the upper 10 cm of the 3 cores also corresponds to the years following invasion of the area by

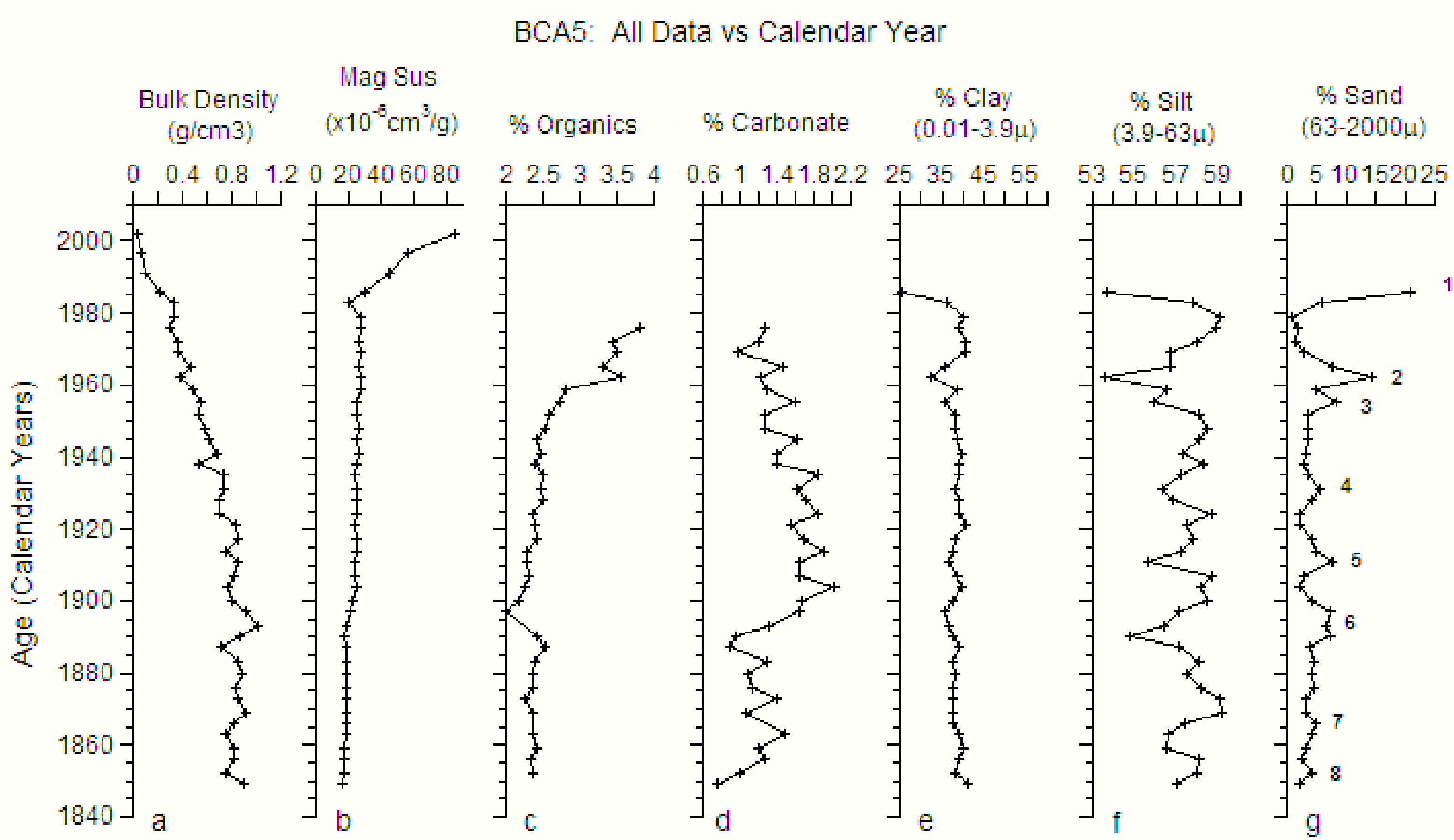

Figure 18: All BCA5 data plotted versus calendar year (numbers indicate peaks coinciding with dated flood events.

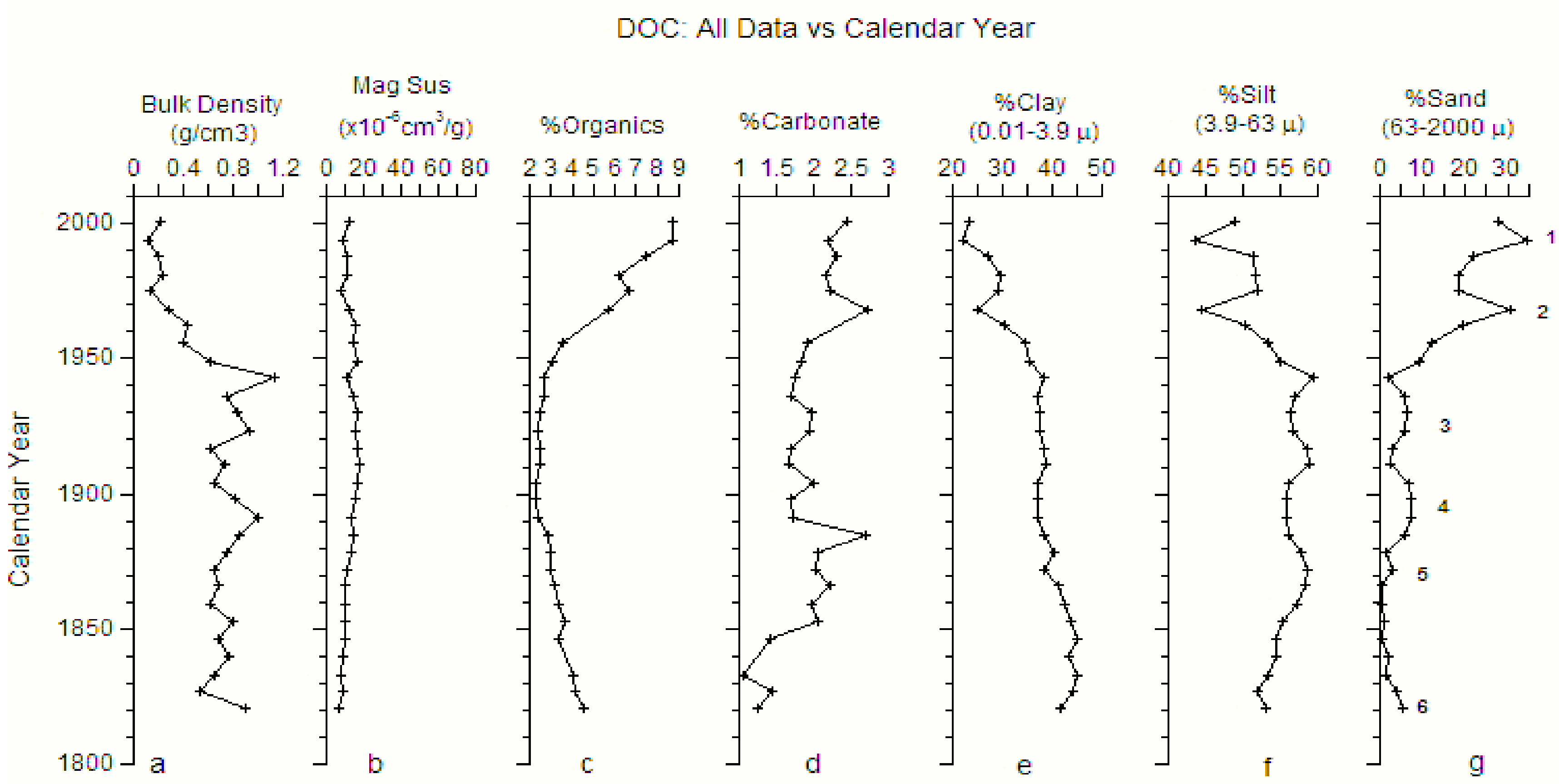

Figure 19: DOC core data plotted versus calendar year (numbers indicate peaks coinciding with dated flood events.)

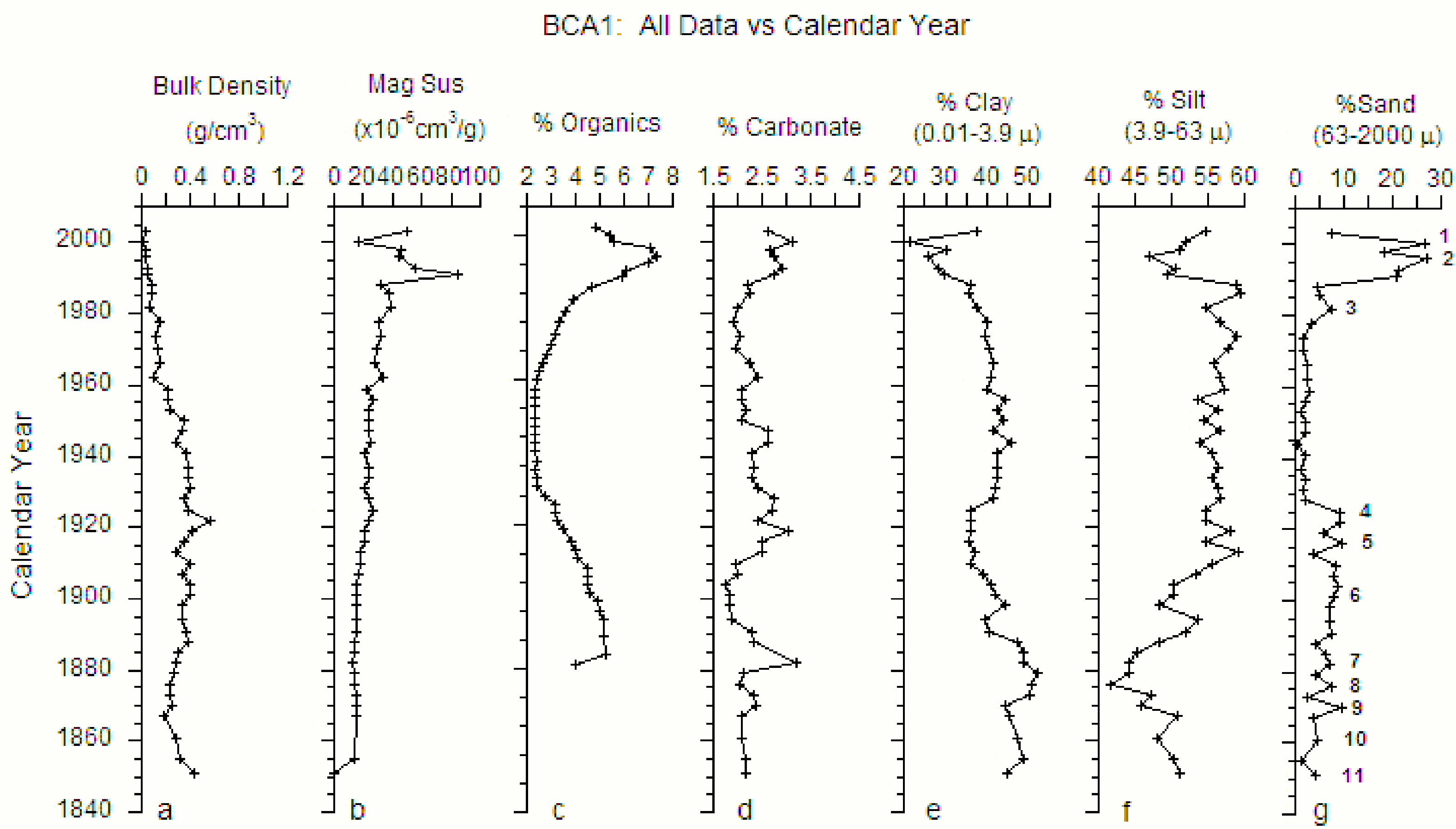

Figure 20: BCA1 core data plotted versus calendar year (numbers indicate peaks coinciding with dated flood events.

Lythrum salicaria in the early 1970s (Figures 18-20). *Lythrum salicaria* grows in large persistent monospecific stands and like many invasive plant species favors the nutrient rich aquatic conditions found in a diked wetland (Herrick and Wolfe, 2005; Thom et al. 2001). Trends in organic matter seem unrelated to changes in other parameters related to flooding and may be more strongly influenced by site effects such as the growth and decay of emergent plant species such as *L. salicaria* as well as spatial variability typical of marsh environments (Alvarez-Cobelas et al. 2007). A possible explanation for the lower percent organic values near the surface of BCA1 could be a decrease in water levels (Figure 20) due to drought or periodic drawdowns, resulting in reduced preservation of organic matter (Wolfe et al. 2005).

Percent carbonate exhibits a weakly-increasing trend between 10 and 30 cm in both BCA1 and BCA5. A similar but slighter increase in percent carbonate is noted in DOC but values decrease sharply below 25 cm. The increased trend in percent carbonate seems unrelated to historically documented flood events but is similar to that observed for bulk density, particularly in BCA5 and BCA1. Peaks in percent carbonate at 28 cm coincide with peaks in bulk density at the same interval in both BCA1 and BCA5, as well at 18 cm in all three cores. Similarities between percent carbonate and bulk density may be related to fluctuations in water levels in the Marsh due to climate fluctuations or human activity. Drying of sediment leads to increased bulk density; decreased water levels can also result in precipitation of Ca and thus higher percent carbonate levels in sediment. Higher Ca content coinciding with increased bulk density values reported by Liu and others (2007) was related to lower water levels. The peaks in percent carbonate near the surface in DOC and BCA1 could also be the result of a drawdown conducted in

2008 as part of marsh management (S. Heerkens, personal communication, April 20, 2009).

Increases in mean grain size are observed as peaks in the sand-sized particle fraction in each core, providing the strongest stratigraphic evidence of past flood events for this study (Figures 18- 21). Increases in mean grain size accompanied by decreases in the percentage of silt and sand-sized particle fractions are indicative of higher energy environments typical of flood events (Wolfe et al. 2006). Huang and others (2007) interpreted peaks in percentages of sand-sized grain fractions within loess-soil sequences as overbank flood deposits. Sant and others (2004) interpreted increases in percentages of >149 µm particle size fractions within unstratified floodplain sediments along the Mahi River as flood deposits associated with strong monsoon events. Peaks in percent sand-sized particles identified within the Marsh cores were compared with dated flood events recorded in historical records and technical reports (Table 1).

Numerous peaks in percent sand-sized particles identified in each of the three cores coincide closely with at least one dated flood event (Table 1). Peaks possibly representing more than one event are designated with an asterisk. BCA1 appears to contain grain-size evidence of at least 9 events (Figure 20), although two of these peaks have yet to be correlated with a documented flood event. Core BCA5 contains evidence of at least eight events but the grain-size record is incomplete due to lack of sufficient sample in the upper 5 cm of the core for the analysis (Figure 18). The compaction of the DOC core during its collection may have reduced the number of discernable peaks in that record (Figure 19).

At least two major flood events are potentially missing from the record constructed in this study. The flood caused by 8 in of rain brought by Tropical Storm Agnes in 1972 might be represented by a significant peak in percent sand in DOC at 6 cm (1968) but such a conclusion is uncertain (Figure 19). During the month of October in 1945 intense rainfall fell at the rate of 4.2 inches in a 24 hr period, producing the most severe flood of record at that time for the Utica area (USACE, 1974; National Oceanic and Atmospheric Administration [NOAA], 2009). This rain event also caused record flows on both the nearby East and West Canada Creeks, nearly destroying the Daniel Greene factory in Dolgeville, New York (NOAA, 2009). Though peaks in bulk density and percent sand appear at this time in DOC (Figure 19), there is no discernible peak in percent sand coinciding with this flood in any of the three cores. Numerous more recent floods occurred during the years 2000-2007 but are unfortunately outside the scope of this study due to loss of the core top during the coring process or due to intentional in-lab combination of the upper few centimeters of the cores necessary to facilitate analysis of the multiple parameters of this study.

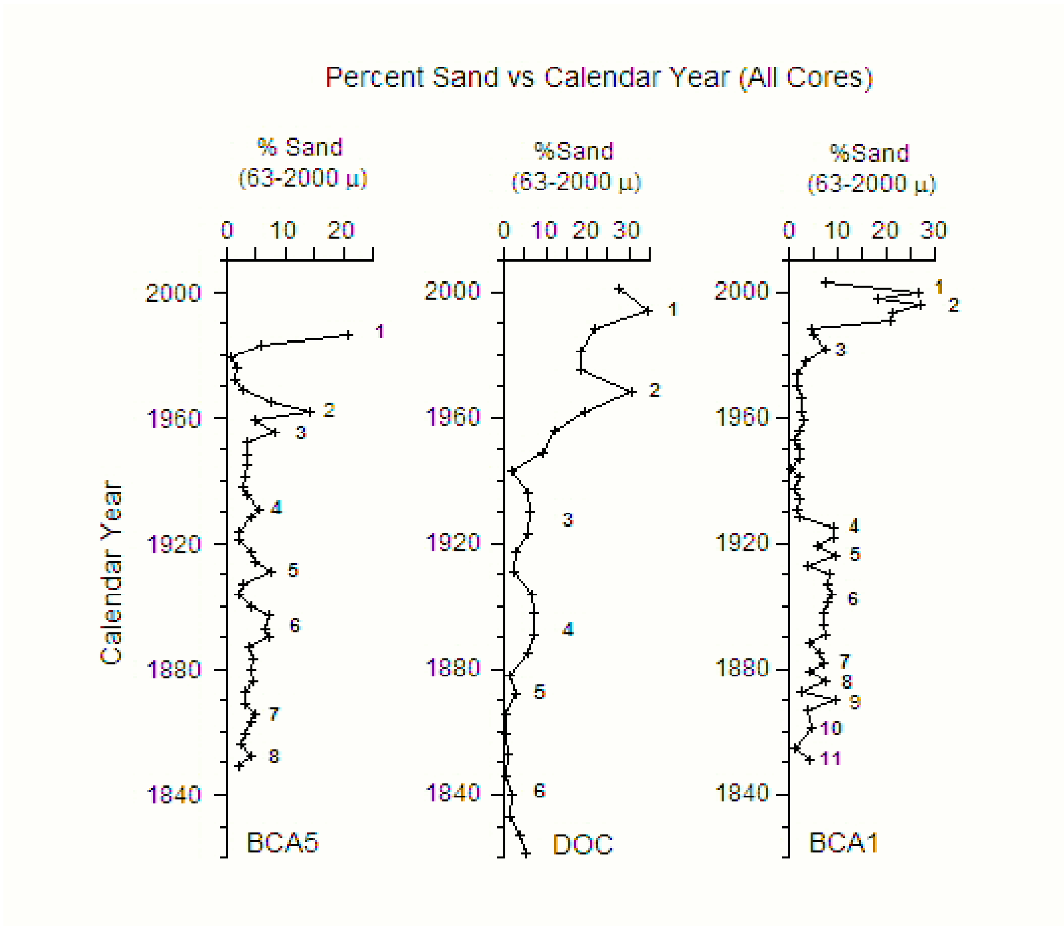

Figure 21: Percent sand plotted versus calendar year (all cores). Numbers indicate peaks coinciding near in time with dated flood events.

Flood Event	Cause	Source	BCA1	DOC	BCA5
Sept, 1999	TS	NO	1		
Jan, 1996	BR	NO,SB	2		
?, 1993	HP	NO, SB		1	
Apr, 1987	?	NO			1
Mar, 1980	HP	NO	3*		
Feb, 1981	IJ	NO	3*		
Apr-May, 1983	HP	NO	3*		
June, 1972	TS	NO, AC		2*	
?, 1970	TS	AC		2*	
?, 1964	IJ	NO, AC			2
Aug, 1955	HU	NO, AC			3
Mar, 1936	HP, SP	NO, AC		3	4
Nov, 1927	HU	NO,	4		
Mar, 1914	IJ	NO, AC	5*		
Mar, 1913	BR, HP	NO, AC	5*		5*
Feb 27-Mar 1,1910	BR?	AC,GG	6*		5*
Oct, 1903	TD	GG	6*	4*	
Mar, 1893	BR	GG	6*	4*	
Feb, 1891	HP,IJ,BR	GG			6
Feb, 1886	BR	GG	7		
?, 1876			8		
Apr, 1870	BR, HP	GG,SC	9*	5	
Oct, 1869	TD, HP	GG, SC	9*		
Mar, 1865	BR, HP	SC	10		7
Sept, 1853	TD	SC	11		8
Nov, 1821	HP	JG		6*	
Mar 3, 1818	HP	JG		6*	
Summer, 1817	HP	JG		6*	

Table 1: Peaks in percent sand (represented by numbers) are correlated with dated events obtained from historical, scientific and technical sources. Peaks possibly representing more than one event are designated by an asterisk. The most extensive record of flood evidence is contained in BCA1. (The sediment record for BCA5 is incomplete due to lack of sample.)

Flood Cause:

HP - Heavy precipitation
BR - Ice Breakup
I J - Ice Jam
HU - Hurricane
TS - Tropical Storm
TD - Tropical Depression

Sources:

NO (NOAA)
AC (Army Corps of Engineers)
GG (Gara and Garver, 2000)
SC (Scheller et al. 2001)
JG (Johnston and Garver, 2000)

Conclusion

Due to its location within the floodplain of the Mohawk River in central New York, sedimentological evidence of inferred flood events is preserved within the Utica Marsh. Grain-size analysis of overbank floodplain sediment records obtained from the three cores reveal shifts in grain-size parameters, particularly increases in sand-sized percentages, indicative of high energy conditions associated with flooding. When compared with historically documented dated flood events, this data suggests floodplain deposits can be used to reasonably reconstruct a history of flooding on the Mohawk River in the Utica area covering the past 185 years. These results further support that such deposits can be used in the reconstruction of a longer record of Mohawk River flooding pre-dating human land use disturbance and anthropogenic climate change in the study area.

The flood reconstructions from the three cores do not match entirely, however, and some of the events are not present in all cores. The selection of another study site within the floodplain less disturbed by human activity would likely provide a more complete sediment record. The use of a larger number of cores would also minimize site effects due to spatial variability of sedimentation and erosion typical of floodplain environments (Walling and He, 1998). It might also overcome problems with radiometric dating due to post-depositional mixing of sediment (Owens et al. 1999). Also, broadening the multi-proxy approach to include tree ring analysis would be more effective in differentiating between changes in the sediment record induced by climate effects such as precipitation variability and those resulting from human influences such as land use (Touchan et al. 2008; Schneider et al. 2007; Van Huissteden and Kasse, 2001).

A longer flooding history is critical to understanding the relative impacts of land use changes (such as agriculture and urbanization) and climate effects on flooding frequency on the Mohawk River. This study suggests that the Utica Marsh data may provide a means to generate such a history, but it also suggests it must be interpreted with caution.

References:

Aerial photo of the Utica Marsh [Online Image]. (n.d.). Retrieved February 16, 2009, http://academics.hamilton.edu/biology/ewilliam/aerial_view.html.

Allguire RL, Cahill RA. 2001. Benchmark Sedimentation Survey of the Lower Cache River Wetlands. [Contract Report 2001-17] prepared for the Illinois Department of Natural Resources.

Appleby PB, Oldfield F. 1978. The calculation of ^{210}Pb dates assuming a constant rate of supply of unsupported ^{210}Pb to the sediment. Catena 5:1-8.

Appleby PG. 2000. Radiometric dating of sediment records in European mountain lakes. Limnology 59 (Suppl. 1): 1-14.

Appleby PG, Dearing JA, Oldfield F. 1985. Magnetic studies of erosion in a Scottish lake catchment. 1. Core chronology and correlation. Limnology and Oceanography 30: 1144-1155.

Albritton, D L, Meira Filho L G. 2001. Climate Change 2001: The Scientific Basis (Technical Summary) [report online] Available at: http://www.ipcc.ch/. Accessed 2008 July.

Alvarez-Cobales M, Sanchez-Carrillo S, Cirujano S. 2002. Strong site effects dictate nutrient patterns in a Mediterranean floodplain. Wetlands 27: 326-336.

Bates BC, Kundzewicz ZW, Wu S, Palutikof JP, Eds. 2008. Climate Change and Water. Technical Paper of the Intergovernmental Panel on Climate Change, IPCC Secretariat, Geneva, 210 pp. Accessed 2008 October.

Benito G, Sopeña A, Sánchez-Moya Y , Machado M, Pérez-González A. 2003. Palaeoflood record of the Tagus River (Central Spain) during the Late Pleistocene and Holocene. Quaternary Science Reviews 22: 1737-1756.

Brenner M, Schelske CL, Keenan L W. 2001. Historical rates of sediment and nutrient accumulation in marshes of the Upper St. Johns River Basin, Florida, USA. Journal of Paleolimnology 26: 241-257.

Coin, G. (2006, Dec 26). Rain ruined canal's season - traffic figures support what officials had suspected after the wet summer. The Post Standard (Syracuse, New York), p.B1. Retrieved February 10, 2009, from NewsBank database.

Collins PEF, Turner SD, Cundy, AB. 2001. High-resolution reconstruction of recent vegetation dynamics in a Mediterranean tidal wetland: implications for site sensitivity and paleoenvironmental research. Journal of Coastal Research 17(3):684-693.

Craft C B and Casey W P. 2000. Sediment and nutrient accumulation in floodplain and depressional freshwater wetlands of Georgia, USA. Wetlands 20: 2, 323-332.

Dean E. 1974. Determination of carbonate and organic matter in calcareous sediments and sedimentary rocks by loss-on-ignition: comparison with other methods. Journal of Sedimentary Petrology 44:242–248.

Dearing J. 1999. Environmental magnetic susceptibility using the Bartington MS2 system. Chi Publishing, Kenilworth, UK.

Del Soccorro Lozano-Garcia, M, Ortega- Guerrero B. 1998. Late Quaternary environmental changes of the central part of the basin of Mexico; correlation between Texcoco and Chalco basins. Review of Paleobotany and Palynology 99:77-93.

Denton GH, Karlen W. 1973. Holocene climatic variations - their patterns and possible cause. Quat. Res. 3, 155-205.

Ely LL, Enzel Y, Baker V R Cayan, D R. 1993. A 5000 year record of extreme floods and climate change in the Southwestern United States. Science 262:410-412.

Estimate flood cost at $375,000. (1972, July 7) Utica Daily Press*,* p.15.

Froelich W, Walling DE. 2007. Predictions in Ungauged Basins: PUB Kick-off (Proceedings of the PUB Kickoff meeting held in Brasilia, 20-22 November 2002). IAHS Publ. 309, 2007.

Gara JJ and Garver JI. 2000. Historical Record of Flooding on the Mohawk River, New York. http://zircon.geology.union.edu/mohawk_river/mohawk_flood
Union College, Schenectady N.Y.

Geiss, CEG. 1999. The development of rock magnetic proxies for paleoclimate reconstruction. (Masters Thesis) University of Minnesota. (http://www.trincoll.edu/~cgeiss/pubs/Thesis/intro.pdf)

Hassan, F A. 1981. Historical Nile floods and their implications for climate change. Science 212: 1142-1145.

Herrick BM and Wolf A. 2005. Invasive plant species in diked versus undiked Great Lakes wetlands. J. Great Lakes Res. 31:277-287.

Huang CC, Pang J, Zha X, Su H, Jia Y, Zhu Y. 2007. Impact of monsoonal climatic change on Holocene overbank flooding along the Sushui River, middle reach of the Yellow River. Quaternary Science Reviews 26: 2247-2264.

Johnston SR, Garver JI. 2000. Major floods on the Mohawk and Hudson Rivers (NY): 1634-1831. Union College.

Jowsey P.C. 1966. An improved peat sampler. New Phytologist 65:245–248.

Kirby ME, Poulsen CJ, Lund SP, Patterson WP, Reidy L, Hammond DE. 2004. Late Holocene lake level dynamics inferred from magnetic susceptibility and stable isotope data: Lake Elsinoe, southern California (USA). Journal of Paleolimnology 31: 275-293.

Knox JC. 2000. Sensitivity of modern and Holocene floods to climate change Quaternary Science Reviews19: 439-457.

Lecce S A and Pavlowsky R T. 2004. Spatial and temporal variations in the grain-size characteristics of historical flood plain deposits, Blue River, Wisconsin, USA. Geomorphology 61:361-371.

Lima AL, Hubeny JB, Reddy CM, King JW, Konrad AH, Eglinton TI. 2005. High-resolution historical records from Pettaquamscutt River basin sediments: 1. ^{210}Pb and varve chronologies validate record of ^{137}Cs released by the Chernobyl accident. Geochimica et Cosmochimica Acta 69:1803-1812.

Liu E, Yang X, Shen J, Dong X, Zhang E, Wang S. 2007. Environmental response to climate and human impact during the last 400 years in Taibai Lake catchment, middle reach of Yangtze River, China. Science of the Total Environment 385: 196-207.

Map of the Utica Marsh Map of the Utica Marsh [Online Image]. (n.d.). Retrieved February 16, 2009, http://academics.hamilton.edu/biology/ewilliam/marsh_map.html

McCarthy, C. (1972, Aug 8). Report on flood damage up-dated. Utica Observer Dispatch, p.25.

National Grid. 2008. Harbor Point Site Remediation Project. Retrieved April 15, 2009 from http://www.harborpointsite.com/SiteDescription.html

National Oceanic and Atmospheric Administration. 2009. Major Flood Events: Eastern New York & adjacent Western New England. Retrieved April 6, 2009, from National Weather Service Forecast Office, Albany, NY Web site: http://www.erh.noaa.gov/er/aly/Past/Major_Flood_Events.htm

Nystrom EA. 2008. Ground-water quality in the Mohawk River Basin, New York, 2006. US Geological Survey Open-File Report 2008-1086, 33p.
Available at http://pubs.usgs.gov/of/2008/1086/pdf/OFR2008-1086.pdf

Oldfield F. 2004. Some personal perspectives on the role of Quaternary science in global change studies. Global and Planetary Change 40: 3-9.

Oneida County, New York. (n.d.). Retrieved February 12, 2009 from Wikipedia the free encyclopedia: http://en.wikipedia.org/wiki/Oneida_County,_New_York.

Owens PN, Walling DE, Leeks GJL. 1999. Use of floodplain sediment cores to investigate recent historical changes in overbank sedimentation rates and sediment sources in the catchment of the River Ouse, Yorkshire, UK. Catena 36:21-47.

Page J N. 1980. Utica Marsh Management Plan. NYS Department of Environmental Conservation Division of Fish and Wildlife (Region 6).

Petit J R, Jouzel j, Raynaud d, Barkov N I, Barnola J M, Basile I, Bendres M, Chappellaz J, Davis M, Delaygue G, Delmotte M, Kotlyakov V M, Legrand M, Lipenkov V Y, Lorius C, Pepin L, Ritz C, Saltzman E, Stievenard M. 1999. Climate and atmospheric history of the past 420,000 years from the Vostok ice core, Antarctica. Nature:399: 429-436.

Porter, S.C., Denton, G.H., 1967. Chronology of Neoglaciation in the North American cordillera. Am. J. Sci. 265, 177-210.

Ramessur RT, Ramjeawon T. 2002. Determination of lead, chromium and zinc in sediments from an urbanized river in Mauritius. Environment International 28: 315-324.

Ritchie JC, McHenry JR. 1990. Application of radioactive fallout for measuring soil erosion and sediment accumulation rates and patterns: a review. Journal of Environmental Quality 19:2-5-233.

Ruggiero K M, Rodbell DT, Garver, J I. 2000. The geological history of Collins Lake, Scotia, New York, as revealed from sub-bottom profiles and sediment core analysis. Union College (http:/zircon.geology.union.edu/Mohawk_river/ruggiero_profile)

Sant D A, Krishnana K, Rangarajan G, Basavaiah N, Pandya C, Sharma M, Trivedi Y. 2004. Characterization of floodplain and climate change using multi-proxy records from the Mahi River Basin, Mainland Gujarat. Journal of Indian Geophys. Union 8:39-48.

Santisteban J I, Mediavilla R, Lopez-Pamo E, Dabrio C J, Ruiz Zapata M B , Garcia J G G, Castano S, Martinez-Alfaro P E. 2004. Loss on ignition: a qualitative or quantitative method for organic matter and carbonate mineral content in sediments? Journal of Paleolimnology 32: 287-299.

Sauquoit Creek Basin Water Management Study. 1996. Vol. 2. p.1.

Scheller M, Luey K, Garver JI. 2001. Major Floods on the Mohawk River (NY): 1832-2000. Union College, Schenectady, New York. http://zircon.geology.union.edu/

Schneider H, Hofer D, Mausbacher R, Gude M. 2007. Past flood events reflected in Holocene floodplain records of East Germany. Geomorphology 92: 208-219.

Thom RT, Borde AB, Richter KO, Hibler LF. 2001. Influence of urbanization on ecological processes in wetlands. Water Science and Application 2: 5-16.

Thompson R. 1975. Magnetic susceptibility of lake sediments. Limnology and Oceanography 20: 687-698.

Touchan R, Meko DM, Aloui A. 2008. Precipitation reconstruction for Northwestern Tunisia from tree rings. Journal of Arid Environments 72: 1187-1896.

United States Army Corps of Engineers. 1974. Flood Plain Information: Mohawk River, Oriskany, N.Y. to Rome, N.Y. US Dept of Defense, Army Corps of Engineers, New York District, 20 pp.

Van Huissteden J, Kasse C. 2001. Detection of rapid climate change in Last Glacial fluvial successions in The Netherlands. Global and Planetary Change 28: 319-339.

Walling DE and He Q. 1998. The spatial variability of overbank sedimentation on river floodplains. Geomorphology 24: 209-223.

Walling DE, Owens PN, Leeks GJL. 1998. The role of channel and floodplain storage in the suspended sediment budget of the River Ouse, Yorkshire, UK. Geomorphology 22: 225–242.

White R W and Rodbell, DT. 2000. A ~1000 Year Record of Sedimentation in Collins Lake as Evidence of Local Storminess and Flooding on the Mohawk River (New York) Union College. http://zircon.geology.union.edu/mohawk_river/white/collins sediment

Whiteley JD, Murray F. 2005. Autocatalyst-derived platinum, palladium and rhodium (PGE) in infiltration basin and wetland sediments receiving urban runoff. Science of the Total Environment 341:199-209.

Williams E, ed. 1990. A Marsh for All Seasons. Utica: Utica Marsh Council.

Winter LT, Foster IDL, Charlesworth SM, Lees JA. 2001. Floodplain lakes as sinks for sediment-associated contaminants- a new source of proxy hydrological data? The Science of the Total Environment 266: 187-194.

Wolfe BB, Karst-Riddoch T L, Vardy S R, Falcone M D, Hall R I, Edwards T W D. 2005. Impacts of climate and river flooding on the hydro-ecology of a floodplain basin, Peace-Athabasca Delta, Canada since A.D. 1700. Quaternary Research 64:147-162.

Wolfe BB, Hall R I, Last ML, Edwards TWD, English M C, Karst-Riddoch TL, Paterson A, Palmini R. 2006. Reconstruction of multi-century flood histories from oxbow lake sediments, Peace-Athabasca Delta, Canada. Hydrological Processes 20: 4131-4135.